Effects of historic and projected climate change on the range and impacts of an emerging wildlife disease

Stephen J. Price[1,2], William T.M. Leung[2], Chris Owen[1], Rob Puschendorf[4], Chris Sergeant[2], Andrew A. Cunningham[2], Francois Balloux[1§], Trenton W.J. Garner[2§], Richard A. Nichols[3§]

[1] UCL Genetics Institute, Darwin Building, Gower Street, London WC1E 6BT, UK

[2] Institute of Zoology, Zoological Society of London, Regents Park, London NW1 4RY, UK

[3] Queen Mary University of London, Mile End Road, London E1 4NS, UK

[4] School of Biological and Marine Sciences, University of Plymouth, Devon, PL4 8AA, UK

Corresponding author: Stephen J. Price (email: *sjamesprice@gmail.com*; Telephone: +447800896114)

§ Balloux, Garner & Nichols should be considered joint senior author

Paper type: Primary Research Article

Running Title: Climate change impacts on a wildlife epidemic

Abstract

The global trend of increasing environmental temperatures is often predicted to result in more severe disease epidemics. However, unambiguous evidence that temperature is a driver of epidemics is largely lacking, because it is demanding to demonstrate its role among the complex interactions between hosts, pathogens and their shared environment. Here we apply a three-pronged approach to understand the effects of temperature on ranavirus epidemics in UK common frogs, combining *in vitro*, *in vivo* and field studies. Each approach suggests that higher temperatures drive increasing severity of epidemics. In wild populations, ranavirosis incidents were more frequent and more severe at higher temperatures, and their frequency increased through a period of historic warming in the 1990s. Laboratory experiments using cell culture and whole animal models showed that higher temperature increased ranavirus propagation, disease incidence, and mortality rate. These results, combined with climate projections, predict severe ranavirosis outbreaks will occur over wider areas and an extended season, possibly affecting larval recruitment. Since ranaviruses affect a variety of ectothermic hosts (amphibians, reptiles and fish), wider ecological damage could occur. Our three complementary lines of evidence present a clear case for direct environmental modulation of these epidemics and suggest management options to protect species from disease.

Keywords: ranavirus, temperature, virulence, climate change, emerging infectious disease, host-pathogen interactions, common frog, *Rana temporaria*, amphibian population decline

1 Introduction

Interactions between hosts, pathogens and their shared environment shape infectious disease outcomes, the timing of outbreaks, and the invasiveness of pathogens (Engering, Hogerwerf, & Slingenbergh, 2013). Climatic conditions at local and landscape scales represent a critical dimension of the host environment - affecting behavior (e.g. aggregation), stress and immunity - but can also directly affect pathogen (and vector) growth and survival (Altizer, Ostfeld, Johnson, Kutz, & Harvell, 2013; Engering et al., 2013; Epstein, 2001; Grassly & Fraser, 2006; Rohr et al., 2011). As such, climatic conditions modulate host-pathogen interactions and operate on multiple timescales: acting annually in driving seasonality (Altizer et al., 2006; Grassly & Fraser, 2006) as well as over longer time periods in determining responses to climate change (Dobson et al., 2015) and influencing the rate and pattern of invasions by emerging pathogens (e.g. Seimon et al., 2007).

Despite this, invasion through pathogen range expansion and environmental change have frequently been viewed as mutually exclusive factors in explaining disease emergence, as indicated clearly in the framing and use of the "novel pathogen" (spread of an exotic pathogen through naïve populations) and "endemic pathogen" (emergence due to perturbations of interaction between hosts and native pathogens) hypotheses (Rachowicz et al., 2005). The "global panzootic" in amphibians caused by the fungal pathogen, *Batrachochytrium dendrobatidis*, serves as a prominent example of how climate change and pathogen range expansion have been pitted against one another as alternative explanations of declines (Berger et al., 1998; Lips, Diffendorfer, Mendelson III, & Sears, 2008; Pounds et al., 2006; Rohr, Raffel, Romansic, McCallum, & Hudson, 2008). There is strong evidence supporting the rapid international spread of a global panzootic lineage of *B. dendrobatidis* during the 20th century

(Farrer et al., 2011; O'Hanlon et al., 2018), but the proposed conflict between the two hypotheses now appears to have been reconciled in a framework that incorporates both as key drivers of emergence and outcomes, explaining observations of decline in regions where the impacts have been greatest (Cohen, Civitello, Venesky, McMahon, & Rohr, 2018; Cohen et al., 2017; Raffel et al., 2013; Rohr et al., 2008). Thus, it seems likely that the previous mindset of treating environmental change and pathogen range expansion as conflicting has hampered understanding of the patterns of emergence and the focusing of mitigation efforts.

Establishing a role for climate in disease emergence can be very challenging. Increasing environmental temperature is a key component of climate change, which is cited as a driver of infectious disease emergence and severity, but evidence for this is scarce and it is often difficult to discriminate between the effect of temperature and other aspects of climate (Harvell et al., 2002). The direct and indirect influences of temperature on host-pathogen interactions (Altizer et al., 2006; Clare et al., 2016; Garner, Rowcliffe, & Fisher, 2011) and its nonlinear effects on incidence and severity (Bosch, Carrascal, Durán, Walker, & Fisher, 2007; Raffel et al., 2013; Walker et al., 2010) represent considerable challenges to a better understanding of disease emergence (Rohr et al., 2011). Most research effort in this area has focused on human diseases (Aguirre & Tabor, 2008), and vector-borne diseases (e.g. malaria, dengue, chikungunya) in particular (Harvell et al., 2002; McMichael, Woodruff, & Hales, 2006).

In the current study, we investigate the effect of temperature on the interaction between ranaviruses and their amphibian hosts, a host-pathogen system that offers the possibility of direct experimental manipulation, and a well characterized recent history of pathogen invasion into the UK (Price, Garner, Cunningham, Langton, & Nichols, 2016). Ranaviruses are large double-stranded DNA viruses (family *Iridoviridae*) that can be highly pathogenic to ectothermic vertebrates (Gray, Miller, & Hoverman, 2009; Price et al., 2014; Rosa et al., 2017). Ranavirus

81 infections of amphibians are notifiable to the World Organization for Animal Health due to their
82 potential to cause severe disease outbreaks as well as the risks of international spread through
83 trade (Schloegel, Daszak, Cunningham, Speare, & Hill, 2010; Schloegel et al., 2009). Ranavirus
84 growth and virulence can be affected by temperature (Ariel et al., 2009; Bayley, Hill, & Feist,
85 2013; Brand et al., 2016; Rojas, Richards, Jancovich, & Davidson, 2005) and environmental
86 temperature is considered to be one possible explanation for observations of seasonality in
87 outbreaks (Brunner, Storfer, Gray, & Hoverman, 2015). Indeed, incidents of ranavirosis in frogs
88 in the USA were recently shown to be uncoupled from a pulse in transmission or the density of
89 susceptible hosts, and instead were coincident with temperature increases and developmental
90 changes in frog larvae (Hall, Goldberg, Brunner, & Crespi, 2018).

91 Ranaviruses are distributed globally but outbreaks of disease are extremely patchy - a pattern
92 which is not yet understood. Some disease outbreaks have been shown to result from human
93 translocations of ranavirus (Jancovich et al., 2005; Picco & Collins, 2008; Price et al., 2016),
94 while other studies have found infections to be widespread at national scales without evidence
95 for disease, which may reflect an historic association (Warne, LaBumbard, LaGrange,
96 Vredenburg, & Catenazzi, 2016; Whitfield et al., 2013). The seasonal patterns and the
97 observations of a temperature effect in laboratory studies raise the possibility that environmental
98 conditions could drive invasion success and routes in cases where ranaviruses are undergoing
99 range expansion as well as climate change being a driver of disease emergence in regions where
100 the associations between viruses and hosts are historic and widespread.

101 In the UK, recurrent amphibian mass-mortality incidents caused by ranavirus have resulted in
102 severe population declines of the common frog (*Rana temporaria*) (Teacher, Cunningham, &
103 Garner, 2010). Genetic evidence supports multiple pathogen introductions into the UK whilst
104 spatiotemporal models suggest that ranavirus spread rapidly, facilitated by translocations of

105 unspecified infectious materials by people (Hyatt et al., 2000; Price et al., 2016). Disease
106 outbreaks are strongly seasonal, peaking in the summer months and appearing to mostly affect
107 adult animals, contrasting with other regions where larvae or metamorphic animals are the worst-
108 affected age-classes (Brunner et al., 2015). However, the detectability of the main UK host, the
109 common frog, is also strongly seasonal and there has been no previous attempts to explicitly
110 control for host population density, host activity or observer effort in examining the periodicity
111 of outbreaks (Cunningham, 2001; Cunningham et al., 1996; Teacher et al., 2010).

112 In this study, we investigated the role of temperature as a driver of disease outbreaks in UK
113 common frogs infected with ranaviruses in the frog virus 3 (FV3) lineage through a combination
114 of epidemiological modelling of a long-term study of disease in wild populations of UK common
115 frogs (Cunningham, 2001; Price et al., 2016), *in vitro* experiments involving manipulation of the
116 host-pathogen environment and similar *in vivo* experiments using natural hosts. Our aims were to
117 examine the role of temperature in shaping host-pathogen interactions to address whether it 1)
118 has been a factor explaining the pattern of invasion which can be used to predict future changes
119 in epidemiology under projections of climate change, and 2) can explain the observed seasonal
120 patterns in disease occurrence and the contrast in affected host age-class compared to other
121 temperate regions experiencing amphibian mortality incidents due to the same type of ranavirus.

2 Materials and Methods

2.1 Temperature as a predictor of frog mortality and incident severity

Temperature-dependence of ranavirus incidence: We used data from the Frog Mortality Project (FMP), a flagship citizen science project which collected information on amphibian mortality incidents for over twenty-five years in order to study disease occurrence in wild populations (Price et al., 2016). The project provided a structured reporting system and guidance to volunteer reporters on how to report amphibian mortality incidents, including a range of variables describing the environment and its management. The FMP dataset has been reliably filtered for incidents of ranavirosis previously (North, Hodgson, Price, & Griffiths, 2015; Price et al., 2016; Teacher et al., 2010) based on detailed post-mortem examinations of dead and sick amphibians reported from multiple sites over multiple years (Cunningham, 2001; Cunningham et al., 1996; Price et al., 2017). In this study, the same criteria as Cunningham (2001) and Price et al. (2016) (the presence of indicative signs of disease [‘ulceration’, ‘red spots on the body’, and ‘limb necrosis/loss of digits’; see Supporting information Appendix S1 and Figure S1] and a minimum of five dead animals) were used to create a binary variable describing the ranavirus status of each incident. To date, no diagnosis other than ranavirosis has been made from pathological examinations of common frogs from such mortality incidents in the UK (Cunningham, 2001; Cunningham et al., 1996; Price et al., 2017). The detectability of amphibians varies seasonally, whilst reporting to the FMP was subject to possible temporal and spatial variation in effort (Price et al., 2016). We controlled for these potential biases indirectly through the inclusion of mortality incidents caused by factors other than ranavirosis as previously (Price et al., 2016). Data on the timing of the onset of mortality (available at the

resolution of month only) and the incident location were used to download the monthly average of the daily maximum temperature (T_{MAX30}) for the month of onset of disease for each incident from the Met Office (Met Office, 2017b) (further details in Supporting information Appendix S2).

Factors affecting ranavirus incidence were investigated using a standard logistic regression model incorporating variables describing the environment (temperature), pond (volume, shading, and presence of marginal and floating vegetation [e.g. see Raffel, Michel, Sites, & Rohr, 2010]), other aquatic vertebrate species present in addition to common frogs (toads, newts, fish) and geographic region (government office region) as predictors of ranavirus status (Model 1) fitted with the R function *glm2* (Marschner, 2011; R Core Team, 2017). To explore the relationship between temperature and the probability of a ranavirus-positive observation further, it was modelled as a sigmoid (logistic) transition between an upper and lower mean frequency (Model 2). The four parameters of the curve (upper and lower limits, the location and the slope of the transition) were fitted using the *mle2* function in the R package, *bbmle* (Bolker & R Core Team, 2017; R Core Team, 2017). Starting values for the *mle2* algorithm were obtained for slope and location (intercept), using the *glm2* function with a bespoke link function for binomial data (Data S2). A confidence interval around the fitted line was generated using the delta method to compute variance of a function with the *emdbook* package (Bolker, 2008, 2016). Model 2 was compared using Akaike's Information Criterion (AIC) to a standard logistic curve (a simplified version of Model 1 with only temperature terms retained as predictors).

Effect of increased temperature on the severity of disease incidents: In order to analyze the effect of temperature on the severity of mortality incidents, the number of dead frogs and the number of surviving frogs (estimated by reporters) at each reported incident were combined as estimates of the proportion of the population that died (each pond/frog population was included

169 in the analysis only once) and used as the response term in a generalized linear model using the
170 quasibinomial family to account for overdispersion in the data (Crawley, 2013). Temperature
171 (T_{MAX30}), the predicted ranavirus status, their interaction, and additional variables which
172 described the pond environment (presence of other species and physical characteristics of ponds)
173 were used as predictors of severity. Since the total number of dead animals at each incident was
174 used to generate the proportion of the population that died when filtering the dataset for
175 ranavirosis-consistent incidents, the criterion requiring mortality incidents to include five or
176 more dead frogs was dropped but the signs of disease data were used more stringently instead
177 (observations of two of the three indicative signs of disease used above were now required).

178 **Temperature preceding ranavirus outbreaks with precise timestamps:** We previously
179 screened a UK amphibian and reptile tissue archive for ranavirus and returned a database of
180 mortality incidents for which the presence of ranavirus was established using molecular
181 diagnostic methods (Price et al., 2017). After filtering for incidents with a precise georeference
182 (postcodes or grid references) and timestamp (date found, submitted, or examined if a post-
183 mortem examination was conducted on receipt, which were each assumed to approximate closely
184 to the day of death due to the rapid decomposition of amphibian carcasses), this dataset
185 contained a total of 197 incidents, for which ranavirus had been detected from 31. All incidents
186 were overlaid on the UK grid of 5 x 5 km squares and the maximum daily temperatures for the
187 date matching the timestamp and the 50 days prior to the death(s) were extracted from plain text
188 data files in the Met Office UK Climate Projections 2009 dataset (Met Office, 2017a), which
189 were downloaded using the R package *Rcurl* (Temple Lang and CRAN team 2018; Price, 2018).

190 Ranavirus status was used as the response variable in a series of logistic regression analyses
191 (generalized linear models using the binomial family and the logit link function) with the average
192 maximum daily temperature in the week preceding the mortality incident (T_{MAX7}) or the number

193 of consecutive days in the previous seven where temperature exceeded 16°C ($DAYS_{T>16}$) as
194 predictors. These models were also run with region (Government Office Region) or latitude as an
195 additional predictor to further control for any effect of spatial variation in temperature. As above,
196 seasonal variation in the detectability of amphibians was controlled for by inclusion of mortality
197 incidents caused by factors other than ranavirosis.

198 **Effects of historic warming and seasonality:** To check whether prior warming (over the time
199 course of the dataset; 1991-2010) had altered the rate of ranavirus incidents and to assess
200 seasonality in the data, we first decomposed the annual signal and trend across years in the time
201 series of temperatures and rates of ranavirosis incidents. The mean of the average daily
202 maximum temperature during the month of onset of mortality incidents from all reports in the
203 FMP dataset (1991-2010) was calculated for each month with reports, as well as the numbers of
204 reports that were consistent or otherwise with ranavirosis. Generalized Additive Mixed Models
205 [GAMM; R function *gamm*; package *mgcv* (Wood, 2003, 2004, 2017)] were used to fit smooth
206 splines to both the within-year (seasonal; cyclic cubic regression spline) and across-year (cubic
207 regression spline) patterns and autocorrelation structures (of order one) were used to model
208 residual correlation within years. The number of ranavirosis incidents as a proportion of total
209 reports was then modeled as a function of the seasonal trend (smoothed with a cubic regression
210 spline as above), the trend in temperature across years (predicted using the GAMM above and
211 smoothed with a cubic regression spline) and time using a Generalized Additive Model (GAM)
212 and the binomial family with logit link function (function *gam*; package *mgcv*).

213 Model assumptions were verified by plotting residuals against fitted values and against each
214 covariate in the model (function *gam.check*; package *mgcv*). Autocorrelation among residuals
215 was assessed using the *acf* function in the *stats* R package (Venables & Ripley, 2002). Model
216 predictions and residuals were extracted and visualized using functions in the R packages, *visreg*

and *ggplot2* (Breheny & Burchett, 2013; Wickham, 2016). The predictive power of the model incorporating the across-year temperature trend was then assessed by comparison to a model containing the temporal trend in the rate of ranavirus incidents by dividing the dataset into two training and test sets (taking half and three-quarters of the data for training respectively). GAMs incorporating the smoothed seasonal trend and either a smoothed (across-year) time trend *or* the smoothed temperature trend were fitted using the training datasets and compared in terms of their ability to predict patterns in the test datasets.

2.2 Virus growth *in vitro*

To investigate the effect of temperature on viral growth, two UK isolates of FV3 [RUK11, isolated from the kidney of a diseased common frog that died with systemic hemorrhages in Middlesex in 1992, and RUK13, isolated from the skin of a diseased common frog that died with skin ulceration in Suffolk in 1995 (Cunningham, 2001)] were grown at a range of temperatures in two cell lines (epithelioma papulosum cyprini [EPC, derived from the fathead minnow fish, *Pimephales promelas* (Winton et al., 2010); ECACC 93120820] and the iguana heart reptile line [IgH2; ECACC 90030804]). Cells were grown on 96 well plates until more than 90% confluent and then inoculated with virus in a ten-fold dilution series ranging from an estimated multiplicity of infection of approximately 2×10^{-6} to 2×10^{3} (five wells per dilution with an additional one well per dilution receiving a sham exposure of cell culture media only as a negative control). Titers of viral isolate stocks were equalized by reference to qPCR scores [following Leung et al. (2017)]. Plates were incubated at six temperatures (10, 14, 18, 22, 26, and 30°C) and monitored daily for cytopathic effect (plaques in the cell layer). After six days, plates were scored for viral growth by counting the number of replicates at each dilution where cytopathic effect was evident and calculating the Tissue Culture 50% Infective Dose (TCID50) using the method of Reed &

Muench (1938). The effects of temperature and cell line on viral growth (the mean titers of the two isolates of each type) were analyzed using a linear model in R.

2.3 *In vivo* assessment of effect of temperature on virulence

To investigate whether an effect of temperature on *in vitro* viral growth was reflected in altered virulence *in vivo*, 60 overwintered common frog metamorphs (*R. temporaria*) were randomly allocated to one of six treatments (10 animals per treatment): three exposure treatments (sham, RUK11, RUK13) crossed with two temperatures (20°C ["low"] and 27°C ["high"]). Temperature was maintained by placing five individually-housed frogs selected at random from each of the three exposure treatments into one of four climate-controlled chambers constructed from polystyrene boxes - two held at 20°C and two held at 27°C (Figure S2; see Supporting information Appendix S3 for a comprehensive description of the set up). RUK13 was used at a titer of 1.58×10^5 TCID50 mL^{-1} and RUK11 at a titer of 1.58×10^7 TCID50 mL^{-1} (see Supporting information Appendix S3 for details of preparation of inocula and exposure methods).

Individuals reaching endpoints (either gross signs of hemorrhaging or ulceration; Figure S1) and all surviving individuals at the end of the experiment (day eight post-exposure) were euthanized following a schedule 1 method for amphibians. The number of hours post-exposure that animals were found dead or at endpoints was recorded for survival analysis. Survival data were analyzed by fitting a mixed-effects Cox proportional hazards regression model in R using the *coxme* package (Therneau, 2018) with exposure and temperature as fixed effects and the climate-controlled chamber as a random effect to account for pseudo-replication due to placement of individual experimental units inside the four climate-controlled chambers.

A second *in vivo* experiment was performed in the same host species, using one ranavirus isolate (RUK13) and a single temperature (20°C), but two exposure doses ("low" and "high"; detailed methods in Supporting Information Appendix S1). The effects of temperature and dose on disease progression and survival were compared.

2.4 Effect of projected climate change on timing of ranavirus outbreaks

Baseline temperature data were generated by calculating the mean daily maximum temperature for each calendar month for the period 1991-2010 (the same period covered by our dataset of reported frog mortality incidents) for each 5 x 5 km grid square used by the Met Office UK Climate Projections 2009 (UKCP09) project (Met Office, 2017b). UKCP09 integrated a range of climate models to predict future climate under the Intergovernmental Panel on Climate Change (IPCC) B1 ("low"), A1B ("medium") and A1FI ("high") future emissions scenarios (IPCC, 2000; Jenkins et al., 2009). Model outputs include probabilities that climatic variables will exceed user-selected values at several future timepoints. We used the threshold temperature from ranavirus occurrence "Model 2" (see section "Temperature-dependence of ranavirus incidence"), at which the risk of ranavirus outbreaks rose sharply, in order to generate probabilities of the mean daily maximum temperature exceeding 16°C for calendar months during the period 2070-2099 for each UK 25 x 25km grid square and under each future emissions scenario. These probabilities were visualized by coloring grid squares on maps based on a probability threshold of 0.5.

3 Results

3.1 Effect of temperature on disease occurrence and severity in the wild

The finalized FMP dataset used in this study contained 4385 unique records, of which 1497 were classed as ranavirosis-consistent. The logistic model (Model 1) revealed a highly significant, non-linear effect of temperature on the proportion of ranavirosis-consistent incidents observed (Table S1). The minimal adequate model also retained newts, fish and shading: the presence of either type of animal in ponds increased the proportion of ranavirosis-consistent incidents observed whilst shading reduced this proportion (Table S1). To explore the relationship with temperature further, a model with a transition between an upper and lower frequency was fitted (Model 2), which improved the fit to the data compared to a simplified version of Model 1 comprising only the terms describing the non-linear relationship with temperature (AIC scores were 5565 and 5576 respectively). Model 2 shows a step-change: below approximately 16°C, 25.1% of incidents were ranavirosis-consistent, rising to 38.5% after the temperature threshold was crossed (Figure 1a). The difference between incidents that were ranavirosis-consistent and the remainder ('non-ranavirus') is also apparent in the distribution of temperature records: the non-ranavirus category being strongly bimodal with peaks at both low and high temperature, whereas most of the ranavirosis-consistent incidents were reported at higher temperatures with few outliers at much lower temperatures (Supporting information Figure S3).

Temperature was again a highly significant predictor of ranavirus status when the records with precise timestamps and confirmed ranavirus-positive status were analyzed. This more precise information about timing enabled a fine-scale examination of the effect of temperature in the

304 days preceding incidents. The average temperature in the seven days preceding incidents (T_{MAX7})
305 was a significant predictor of ranavirus status (odds ratio = 1.20, 95% confidence interval = 1.09
306 – 1.31; Figure 1b). The temperature threshold where the proportion of ranavirus incidents
307 increased sharply in the analysis of the full FMP dataset (Model 2) was approximately 16°C. A
308 second model - with the number of consecutive days where the daily maximum temperature in
309 the week preceding incidents exceeded 16°C ($DAYS_{T>16}$)as a predictor - also indicated that
310 warmer temperatures were a good predictor of ranavirus status with each additional warm day
311 raising the odds that incidents were caused by ranavirus (odds ratio = 1.33, 95% confidence
312 interval = 1.16 – 1.51; Figure 1c). The 16°C threshold model had a slightly lower AIC score than
313 the model using the average temperature as a predictor (155 compared to 158).

314

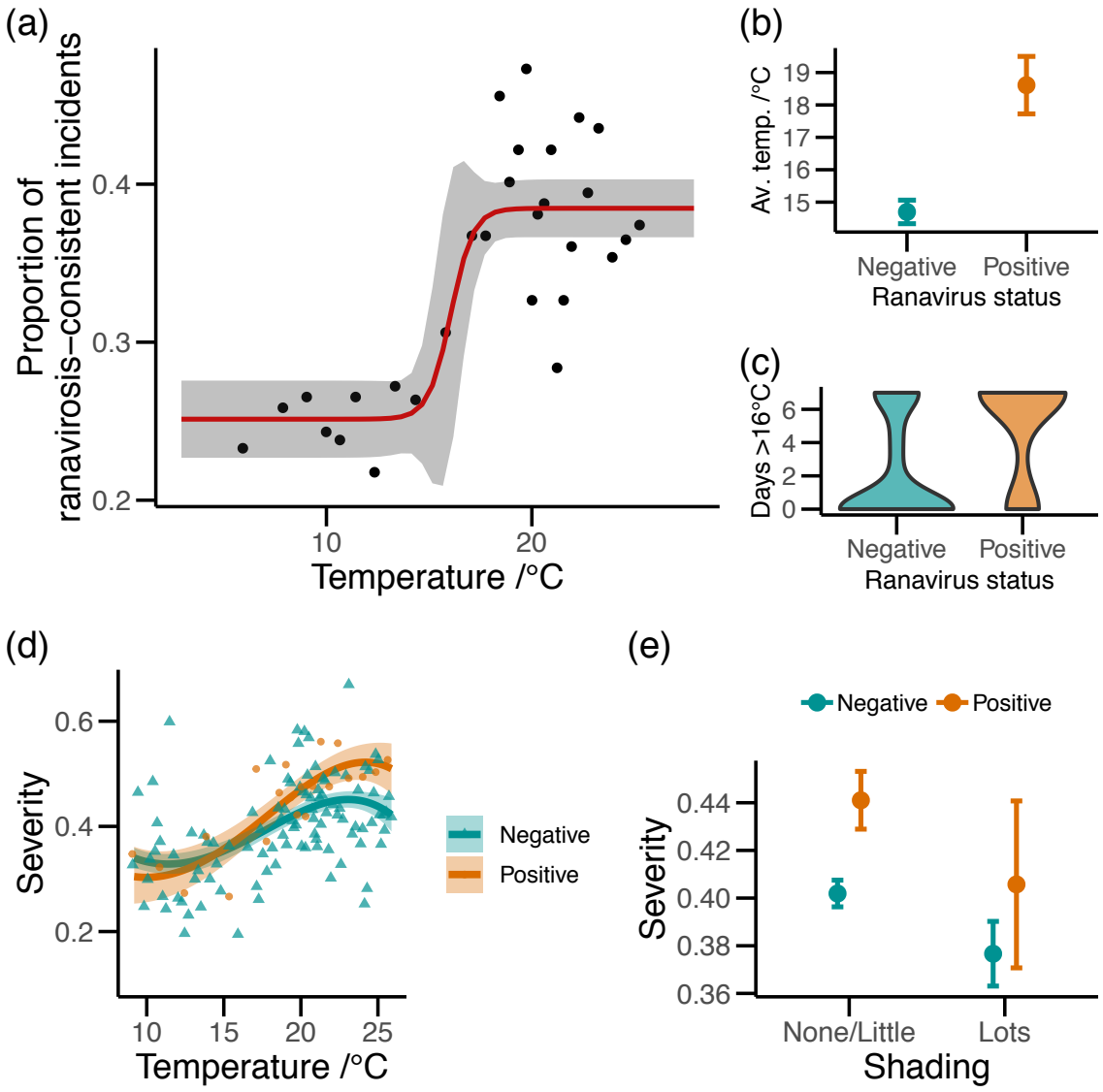

315

316 **Figure 1. Warm temperatures increased the frequency and severity of incidents of**
317 **ranavirosis involving wild common frog populations of the United Kingdom.** (a) The effect
318 of temperature on ranavirosis incident rate (the proportion of citizen science reports of frog
319 mortality that were classified as ranavirosis-consistent). The line represents the fitted maximum
320 likelihood model of a logistic transition between a lower and upper frequency. The shaded area
321 around the line represents the 95% confidence interval, calculated using the delta method. Points

represent the observed data, grouped in 30 windows each containing 146-148 individual records. (b-c) Temperature in the week preceding frog mortality incidents confirmed by molecular methods predicted ranavirus status ("Positive" or "Negative"). (b) T_{MAX7} by ranavirus status. (c) $DAYS_{T>16}$ by ranavirus status. (d) The severity of frog mortality incidents (estimated proportion of population that died) was consistently greater at higher temperatures, particularly in the case of ranavirosis-consistent incidents (orange). The plot shows fitted lines (and 95% confidence intervals) from a generalized linear model (quasibinomial regression) of severity as a function of ranavirus status and temperature (T_{MAX30} for the month of onset of mortality incidents, including quadratic terms). Points are a summary of raw data after binning individual data points (mode of twenty data points per bin) and calculating the mean temperature and overall proportion of dead frogs within each bin. (e) Large amounts of shading around ponds reduced the severity of ranavirosis-consistent mortality incidents (orange) compared to other incidents (green). In panels (b) and (e), points represent means and error bars represent ±1 standard error of mean.

The FMP database contains data on the severity of outbreaks (the estimated proportion of the frog population that died) for the years 1991-2000. After removing records with missing values, we produced a dataset for investigating severity that contained 2667 records, of which 427 incidents were classified as ranavirosis-consistent. The effects of temperature and covariates previously identified as having an influence on the occurrence or severity of ranavirosis in UK common frogs (North et al., 2015) were explored using a logistic model. The ranavirus status and temperature (T_{MAX30} at month of mortality onset) plus their interaction, as well as the log-transformed pond volume, shading around ponds, the amount of both the marginal and floating vegetation ("none/little" or "lots"), the presence of toads, the presence of newts, the presence of fish, and the region were all included as predictors in the model. After model simplification, the

minimal adequate model retained temperature, ranavirus status and their interaction but there were also significant effects of the presence of toads, the presence of fish, shading, pond volume (non-linear), marginal vegetation and region (Table S2). Temperature had a significant, positive effect on incident severity, each 1°C increase in temperature leading to a 3.1% increase in the proportion of the population that died ($p = 7.56 \times 10^{-12}$). There was a significant interaction with ranavirus status ($p = 7 \times 10^{-4}$): at low temperatures, the severity of ranavirosis-consistent incidents was lower than other types of incident but at higher temperatures ranavirosis-consistent incidents were more severe (Figure 1d; Supporting information Figure S4). Toads reduced the severity of mortality incidents whilst the presence of fish increased severity (Supporting information Figure S5) as found previously (North et al., 2015). Shading and marginal vegetation decreased the severity of incidents. Notwithstanding, and irrespective of which covariate was considered, the effect of increasing temperature increased the severity of disease. This is perhaps best illustrated by the effects of pond shading, where increasing the amount of shading (and, presumably, decreasing the maximum temperatures that frogs would have been exposed to) was associated with reduced severity of ranavirosis and a reduction in the disparity in the severity of incidents between ranavirosis-consistent and non-ranavirus incidents (Figure 1e).

3.2 Historic climate change and seasonality

Temperatures in our study region varied across years, showing a warming trend that peaked in 2002 before cooling up to 2010, as well as showing marked seasonality (GAM component of GAMM: $R^2 = 0.93$; Table S3). The proportion of ranavirosis incidents followed a remarkably similar pattern, in terms of the strong seasonality and the trend across years (GAM component of GAMM: $R^2 = 0.36$; Table S4; Figure 2a). The across-year temperature trend was a highly significant predictor of the rate of ranavirus incidents (GAM: effective degrees of freedom (edf)

of smoothed term = 6.65, p = 4.61×10^{-26}), explaining the pattern of increasing rates which peaked in 2001, with the full model explaining approximately half the deviance (R^2 = 0.48; Figure 2; Table S5). Model validation indicated conformity to assumptions. The temperature model, when trained on subsets of the data, predicted trends in test datasets effectively in contrast to models incorporating only the across-year trend in ranavirosis rates, which showed no predictive power (Supporting information Figure S6). Temperature showed a strong seasonal pattern which was reflected in the pattern of ranavirosis incidents where seasonality was also marked (GAM: edf = 7.65, p = 2.45×10^{-13}; Figure 2c). Overall, after accounting for the effect of temperature, there was a small but significant decrease in the proportion of ranavirosis incidents between 1991 and 2010 (GAM: coefficient = -0.00315 [unit of time was months], p = 2.31×10^{-5}; Figure 2d).

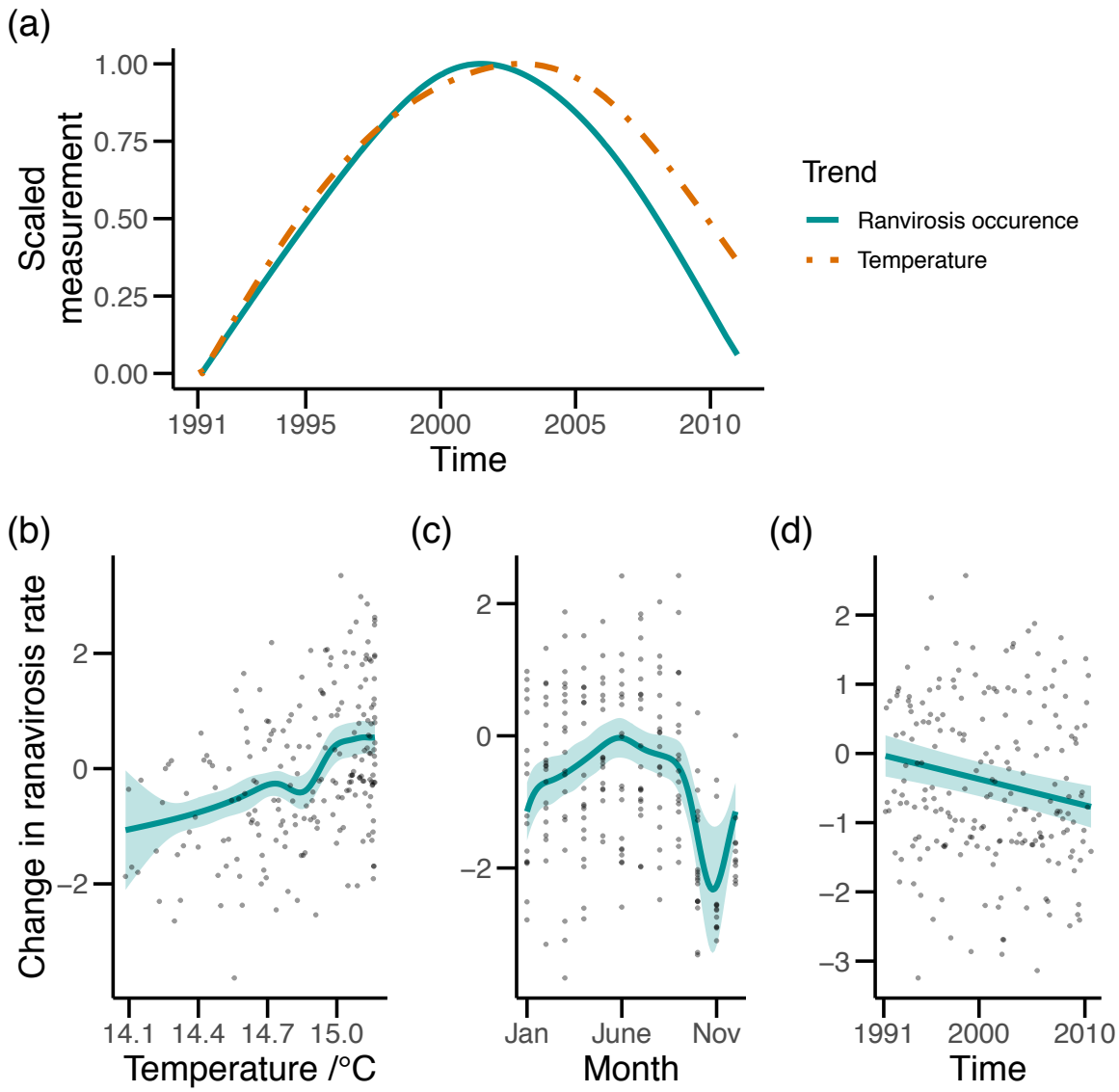

380

381 **Figure 2. Effect of historic climate and seasonality on rate of ranavirosis incidents.** (a)
382 comparison of smoothed trends in temperature and rates of ranavirosis incidents (on standardized
383 scale [0-1]) over period of dataset (1991-2010). (b-d) Effect of predictors of the rate of
384 ranavirosis incidents (from generalized additive model) against residuals: Smoothed change in
385 rate of ranavirus incidents with temperature (b), smoothed seasonal change in rate of ranavirosis
386 incidents (c), and change in rate of ranavirosis incidents over time (d). Shaded areas represent
387 95% confidence intervals.

3.3 *In vitro* assessment of viral growth rates and *in vivo* tests of virulence

We examined *in vitro* viral growth using two UK isolates of FV3 (RUK11 and RUK13; see methods for detailed descriptions of isolates) and two cell lines. Each isolate was incubated at a range of temperatures up to 30°C with each cell line, but regardless of cell line or isolate, increasing temperature resulted in exponentially increased rates of plaque formation (Figure 3). A linear model of log viral titers against temperature, cell line and their interaction revealed significant effects of temperature (coefficient = 1.23, $p < 1e^{-30}$) and host cell line (IgH2 compared to EPC, coef = -8.64, $p < 1e^{-30}$) but no interaction (analysis of variance, comparing model with interaction term to a model with main effects only: $F_{df=1} = 0.0047$, $p = 0.95$).

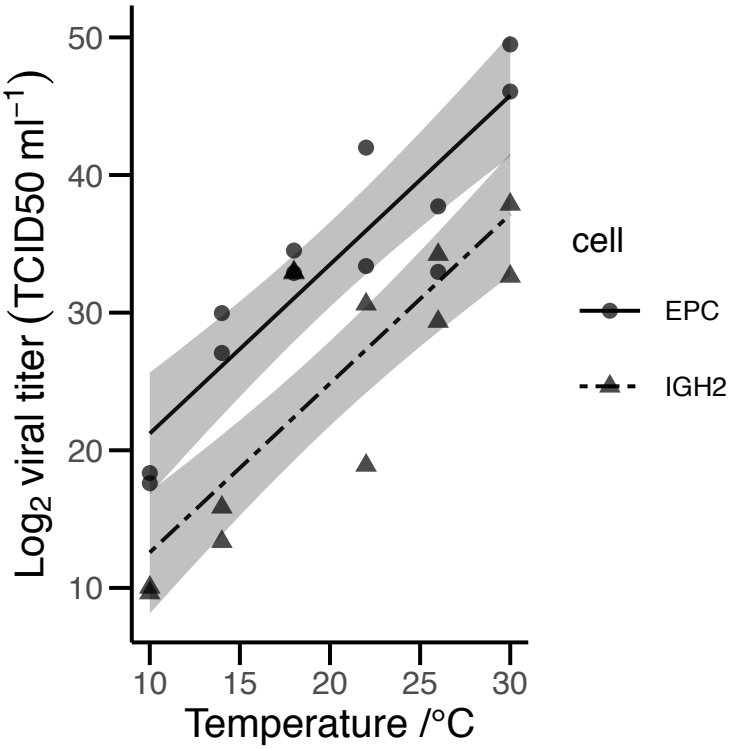

399

400 **Figure 3. Effect of environmental temperature on growth of UK *Frog virus 3* (FV3) *in vitro*.**
401 Observed data (points) and predictions from linear model (lines with 95% confidence interval
402 shaded) of FV3 growth at a range of environmental temperatures in fish (EPC; solid line) and
403 reptile (IgH2; dashed line) cells. Growth was measured using the TCID50 method and is shown
404 on a log scale. An increase in temperature of 1°C results in more than a doubling of viral growth
405 (2.34 times).

406

407 The effect of temperature on the response of common frogs to viral exposure was assessed in
408 order to validate results from cell culture models *in vivo*. Temperature was a highly significant
409 predictor of survival: 20 of 60 animals died or were euthanized on reaching humane endpoints,
410 of which 14 were from high temperature treatments and six were from low temperature

411 treatments (Figure 4). Overall there was a 5.33 times higher risk of death in the high temperature
412 treatments ($p = 0.005$; Table 1). Titers of viral inoculates were not equalized between isolates.
413 All individuals exposed to RUK11 (at a high dose) and maintained at high temperature died or
414 reached endpoint by the eighth day post-exposure compared to six of ten individuals maintained
415 at low temperature (Figure 4). Of the animals exposed to RUK13 (at a relatively low dose
416 compared to RUK11), three individuals died or reached endpoint in the high temperature
417 treatment compared with none at the low temperature. There was also a significant effect of
418 exposure treatment: the expected hazard of animals exposed to RUK11 was 41.6 times higher
419 than animals receiving a sham exposure ($p = 0.0004$). These results are largely in line with a
420 study examining survival of common frog tadpoles exposed to a North American isolate of FV3,
421 which showed that mortality was increased at 20°C compared to 15°C (Bayley et al., 2013).

422 The second *in vivo* experiment examining the effect of dose on disease outcome and progression
423 in juvenile common frogs (Supporting Information Appendix S1) complements the findings of
424 the *in vivo* temperature experiment. The dose experiment suggests that a viral load threshold
425 exists which must be crossed before gross signs of disease develop. We found the outcome and
426 presentation of disease as well as the viral quantity in tissues at death to be largely independent
427 of dose: all animals exposed to either low or high viral doses died, presented with the same set of
428 signs (Figure S1 & S7), and had similar quantities of virus in their tissues at death (Figure S8a).
429 However, the onset and progression of disease was delayed at low dose (the development of
430 disease and death both occurred significantly later; Figure S7) reflecting the lower viral loads of
431 individuals (measured by swabbing animals after infection; Figure S8b) in this treatment. Also,
432 viral loads of dead individuals were greater than those of live individuals (both when repeated-
433 measures from the same individuals were compared [Figure S8c] and when individuals that were
434 euthanized part-way through the experiment were compared to those that died [Figure S8d]).

These results all suggest that elevated viral loads lead to the onset of disease and that the viral capacity to cross a threshold concentration is a more important determinant of whether disease develops than the initial dose. It seems likely that higher temperature and higher initial dose each serve as ways to reach this putative threshold for disease sooner - either through more rapid viral growth or a greater initial intensity of infection respectively - and explain the delays and/or reductions in observations of severe outcomes in the other respective treatments (low temperature or low dose).

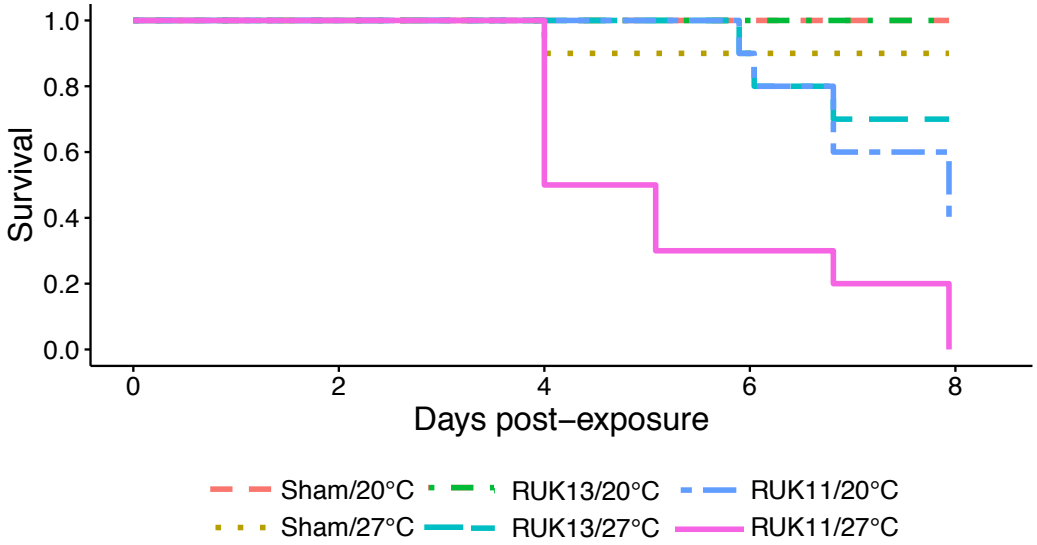

Figure 4. Effect of temperature and ranavirus exposure on survival of common frogs. Kaplan-Meier survival plot showing the proportions of surviving animals through time plotted for each of six treatments (n=10 frogs per treatment); three exposure treatments (Sham, RUK11, RUK13) at each of two temperatures (20°C [“low”] or 27°C [“high”]).

Table 1. Effect of temperature and ranavirus exposure treatments on the survival of common frogs. Coefficients and hazard ratios from a mixed effects Cox Proportional Hazards model of survival in response to exposure ("Sham" as the reference level) and temperature ("Low" as the reference level) treatments.

	Coefficient	Hazard ratio (e^{coef})	Standard Error	z-value	p-value
RUK13 exposure	1.17	3.23	1.16	1.01	0.310
RUK11 exposure	3.73	41.6	1.05	3.56	<0.001
"High" temperature (27°C)	1.67	5.33	0.59	2.84	0.005

3.4 Impact of future climate on timing of outbreaks

The UK climate is expected to warm considerably over the remainder of the century (Chen & Tung, 2018; Jenkins et al., 2009). A warmer climate would expand the geographic area where environmental conditions are likely to be suitable for severe incidents of ranavirosis (T_{MAX30} exceeding 16°C; Model 2). For example, using 16°C as the point value where the risk of ranavirosis outbreaks increases, the suitable geographic area for ranavirosis occurrence in May is projected to increase by 134% by 2070 under a high emissions scenario compared to the historic baseline and by 84% under a low emissions scenario (Figure 5). The projected changes in UK temperatures are also likely to extend the duration of the "disease season", creating favorable conditions for disease during the spring and autumn as well as in the summer. Temperatures are likely to become more suitable for severe outbreaks in a large part of England in April under a high emissions scenario and in October under any of the range of IPCC scenarios investigated. These are months that we expect to have experienced limited incidence and severity of ranavirosis previously, but temperatures are projected to change to such a degree that this limitation will be removed for large areas of the UK (Figure 5).

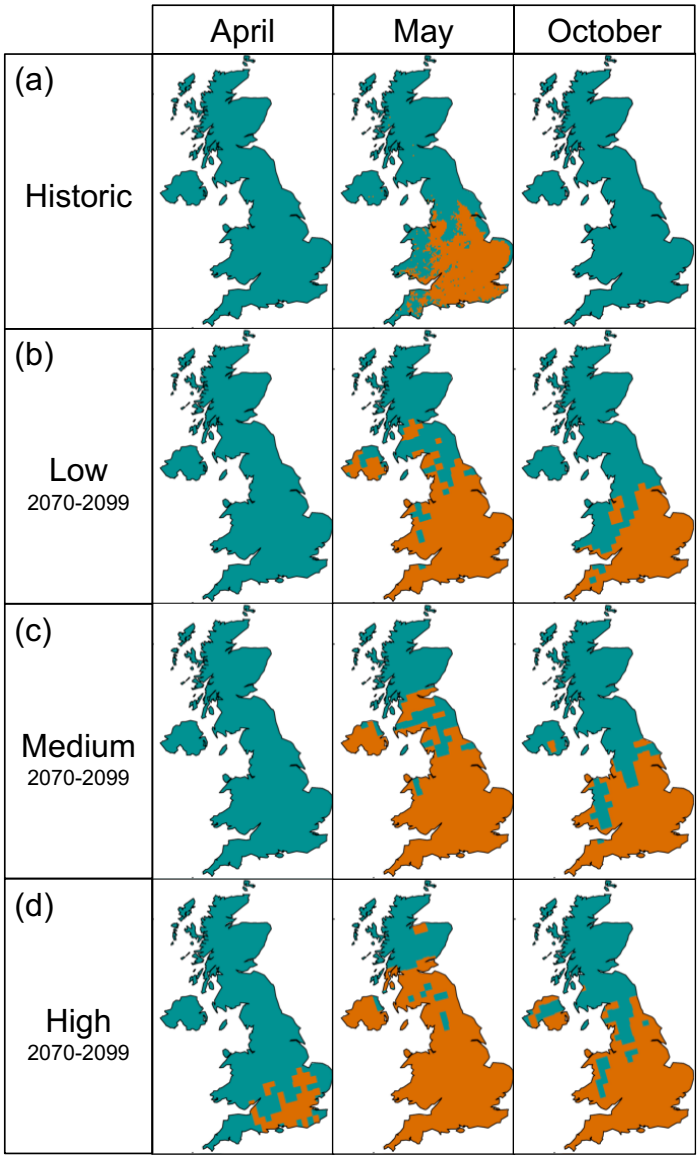

469

470 **Figure 5. Projected shifts in geographic extent and the temporal window of ambient**
471 **temperatures high enough to increase the risk and severity of ranavirosis incidents in the**
472 **UK under different emissions scenarios.** (a) Past climate - orange regions are those where the
473 average monthly temperatures (daily maximum temperature) in the UK (5 x 5 km grid squares)
474 exceeded 16°C for the period 1991-2010. (b-d) Future climate - orange regions are those where
475 the projected average monthly daily maximum temperatures in the UK (25 x 25 km grid squares)

have a greater than 50% probability of exceeding 16°C under a range of future emissions scenarios for the period 2070-2099: (b) Intergovernmental Panel on Climate Change (IPCC) scenario B1 (low), (c) scenario A1B (medium) and (d) scenario A1FI (high).

4 Discussion

By combining the results of laboratory experiments with the analysis of two types of epidemiological dataset relating to disease outbreaks in wild amphibian populations, we have revealed a pattern of remarkably consistent evidence supporting a strong, positive effect of temperature on the occurrence and severity of ranavirosis in UK common frogs. Temperature predicts both the incidence and severity of disease outbreaks through higher temperatures increasing viral growth which, in turn, manifests as an increased rate of disease occurrence in both experimental and wild frog populations. Temperature is, of course, correlated with a multitude of other factors that may be considered alternative or additional drivers of disease outbreaks. That seasonal patterns were found in ranavirosis occurrence as well as temperatures raises the possibility that another seasonal factor - correlated with temperature - could have driven ranavirosis outbreaks. However, temperature was associated with disease incidents at two different timescales (within and across years). The association between temperature and the rate of ranavirus incidents across years suggests that temperature is driving the rate of disease incidents in the long term and may also drive the seasonality, since both a correlated seasonal factor and a correlated non-seasonal factor acting across years would otherwise be required to explain the observed patterns. Furthermore, the use of *in vitro* and *in vivo* studies in combination with modeling of field datasets serves as a 'triangulation' process (Plowright, Sokolow, Gorman,

498 Daszak, & Foley, 2008) and strongly suggests a causal link between temperature and disease
499 occurrence in this system.

500 Our results are consistent with an historic effect of climate on the rate and timing of ranavirus
501 incidents and suggest that the invasiveness of this introduced pathogen may have been
502 influenced by the suitability of local climate. We have previously shown that ranavirus was
503 introduced to the UK and spread rapidly in England (Price et al. 2016). The small overall
504 decrease in the rate of disease incidents observed over the twenty years of data analyzed, which
505 was observed after controlling for the effect of temperature (Figure 2d), may be due to fewer
506 opportunities for spread arising from a more complete colonization of the suitable range or might
507 be explained by efforts to limit the risk of translocations through advice disseminated in the
508 media (e.g. BBC, 2008; Price et al., 2016). Alternatively, the severe impacts of recurrent
509 ranavirus outbreaks - previously shown to have caused declines of common frogs in South-East
510 England (Teacher et al., 2010) - might have led to the extirpation of populations or reduced their
511 size/density to the point where transmission no longer occurred, or disease outbreaks were no
512 longer detectable.

513 Climate projections were focused on the temporal and spatial changes in the suitable region for
514 outbreaks of ranavirosis but use a single point value from a regression model and therefore do
515 not capture uncertainty around the temperature threshold for increased risk. However, the
516 projections illustrate that any degree of climate change will likely play a role in shaping future
517 ranavirus disease dynamics in UK common frogs, altering both the geographic extent and the
518 length of the temporal window of heightened disease risk and severity. The potential impacts of
519 climate warming on disease ecology, therefore, could have critical ramifications for the
520 continued survival of amphibian populations across the UK.

Although it is challenging to detect disease and mortality in larval amphibians, all evidence points to adult common frogs as the major life history stage and species affected by ranavirosis in the wild in the UK (Cunningham, 2001; Duffus, 2009; Price et al., 2017). This observation is intriguing since larval forms are usually more affected by FV3 elsewhere in the world and common frog larvae have been shown to be highly susceptible to wild-type ranaviruses in the laboratory (Duffus, Nichols, & Garner, 2013; Duffus, Nichols, & Garner, 2014; Gray et al., 2009). Our findings suggest that temperature could be an important determinant of the partitioning of disease among life-history stages, with common frog larvae metamorphosing before pond water reaches a temperature high enough to trigger outbreaks of ranavirosis. This situation could be altered as the climate warms and the disease season is lengthened. Shifting the timing of frog disease outbreaks will alter the life history stages at risk. If common frog tadpoles become affected, the abundance of susceptible hosts will be increased with concomitant impacts on the ranavirus basic reproductive number (R_0) (Altizer et al., 2006); i.e. the dynamics of outbreaks will be fundamentally changed, making predictions of their impacts more challenging.

Additional research on the effect of climatic changes on the breeding phenology of UK amphibians is needed, but it has been suggested that the common frog differs from other UK species in having shown no response in the timing of breeding to increasing absolute temperatures (Beebee, 1995). Therefore, any compensatory changes in common frog behavior to future climate change may be negligible. Common frog populations in regions where temperatures become suitable for severe disease outbreaks during the larval stage might experience reduced recruitment and a subsequent reduction in their capacity to persist in the presence of infection. Additionally, altering the timing of outbreaks could create opportunities for host jumps if other potential host species have increased contact with (high levels of) virus (Hoberg & Brooks, 2015). The results highlight how species with complex life cycles might

undergo sudden shifts in the level of threat posed by an infectious disease if gradual changes to the climate result in greater exposure/susceptibility of alternative life history stages when a favorable environment had previously buffered them against the most severe impacts of disease. However we did not have information about the inflection point in the viral growth curve or how frog populations will respond if temperatures exceed such an inflection point, so predictions of how individual outbreaks would proceed through the whole season were not attempted and it is possible that impacts might be reduced in some populations due to exposure to very high temperatures in the future.

Our laboratory findings that virulence is reduced at lower temperatures, that frogs might be better able to manage infections at lower temperatures, together with field records showing a mitigating effect of shading, pond volume and vegetation (which might also be due to lowered temperatures of frogs) on incidence and severity of ranavirosis, point to possible steps for mitigation. Thermoregulatory behavior leading to an increase in body temperature above normal range ("behavioral fever") is known to be important for disease mitigation in a range of ectotherms (Boltaña et al., 2013; Elliot, Blanford, & Thomas, 2002; Monagas & Gatten, 1983). Whether thermoregulatory behavior serves as an amphibian strategy for managing infections remains to be elucidated (Sauer et al., 2018) but shading has been proposed as an environmental feature that might have negatively impacted the ability of newts to clear chytrid infections because it limited the availability of warm-water patches (Raffel et al., 2010). Staying cool can be a more difficult challenge than getting warm for many ectotherms (Kearney, Shine, & Porter, 2009), but the provision of suitable opportunities for behavioral regulation of body temperature in the form of shading, log piles and larger ponds might help to manage the severity of future outbreaks and warrants further study.

568 Ranavirosis has had a major impact on common frog populations in south-east England (Teacher
569 et al., 2010) and the current study suggests that these impacts may become greater and more
570 widespread (in the UK and elsewhere) if future climate change projections are realized. Our
571 results - as well as the predictions that follow from them - are strengthened through the use of a
572 model system that allows us to investigate possible drivers of field epidemiology using
573 laboratory experiments, both at the cellular and whole animal levels. Together, our results
574 present a clear case of the environment modulating an important host-pathogen interaction. Few
575 previous studies have convincingly shown how climate change affects disease emergence in wild
576 animal populations, but we have been able to demonstrate a historic impact of warming in the
577 wild and then tease apart relationships between the environment, host and pathogen in the
578 laboratory. These results underline the importance of accounting for the effects of local
579 environmental drivers to predict the dynamics of an invading pathogen (Cohen et al., 2018,
580 2017; Raffel et al., 2013).

Acknowledgements

We thank Rob Knell for help and advice about climate-chamber construction. This work was funded by NERC grants NE/M000338/1, NE/M000591/1 & NE/M00080X/1. All *in vivo* experimental procedures and husbandry methods were approved by the ZSL Ethics Committee before any work was undertaken and procedures were performed under UK Home Office licenses P8897246A & 80/2214. The authors declare that there are no conflicts of interest. All data and code required to reproduce the analyses in this article are included in the Supporting information files (Data S1 to Data S8).

Author contributions

SJP & AAC designed the *in vitro* experiments, the lab work was performed by CO & WL, and analysis was performed by SJP with help from CO. SJP designed the *in vivo* experiments with help from TWJG & RAN, the lab work was performed by SJP, WL & CS, and the results were analyzed by SJP. AAC oversaw collection of the epidemiological datasets, SJP, RP, TWJG, RAN & FB planned the analyses which were conducted by SJP and RAN. SJP and RP planned the climate change projections, which were performed by SJP. SJP & FB wrote the first draft of the manuscript which was edited by all authors.

References

Aguirre, A. A., & Tabor, G. M. (2008). Global factors driving emerging infectious diseases. *Annals of the New York Academy of Sciences*, *1149*, 1–3. https://doi.org/10.1196/annals.1428.052

Altizer, S., Dobson, A., Hosseini, P., Hudson, P., Pascual, M., & Rohani, P. (2006). Seasonality and the dynamics of infectious diseases. *Ecology Letters*, *9*(4), 467–484. https://doi.org/10.1111/j.1461-0248.2005.00879.x

Altizer, S., Ostfeld, R. S., Johnson, P. T. J., Kutz, S., & Harvell, C. D. (2013). Climate Change and Infectious Diseases: From Evidence to a Predictive Framework. *Science*, *341*(6145), 514–519. https://doi.org/10.1126/science.1239401

Ariel, E., Nicolajsen, N., Christophersen, M.-B., Holopainen, R., Tapiovaara, H., & Jensen, B. B. (2009). Propagation and isolation of ranaviruses in cell culture. *Aquaculture*, *294*(3-4), 159–164. https://doi.org/10.1016/j.aquaculture.2009.05.019

Bates, D., Mächler, M., Bolker, B., & Walker, S. (2015). Fitting Linear Mixed-Effects Models Using lme4. *Journal of Statistical Software*, *67*(1), 1–48. https://doi.org/10.18637/jss.v067.i01

Bayley, A. E., Hill, B. J., & Feist, S. W. (2013). Susceptibility of the European common frog Rana temporaria to a panel of ranavirus isolates from fish and amphibian hosts. *Diseases of Aquatic Organisms*, *103*(3), 171–183. https://doi.org/10.3354/dao02574

BBC. (2008, March 7). Warning against moving frogspawn. Retrieved July 4, 2018, from http://news.bbc.co.uk/1/hi/uk/7282649.stm

Beebee, T. J. C. (1995). Amphibian breeding and climate. *Nature*, *374*, 219–220.

Berger, L., Speare, R., Daszak, P., Green, D. E., Cunningham, A. A., Goggin, C. L., … Parkes, H. (1998). Chytridiomycosis causes amphibian mortality associated with population declines in the rain forests of Australia and Central America. *Proceedings of the National Academy of Sciences of the United States of America*, *95*(15), 9031–9036. https://doi.org/10.1073/pnas.95.15.9031

Bolker, B. (2008). *Ecological Models and Data in R*. Princeton University Press.

Bolker, B. (2016). Emdbook: Ecological Models and Data in R (Version R package version 1.3.9).

Bolker, B., & Team, R. C. (2017). *Bbmle: Tools for General Maximum Likelihood Estimation*. Retrieved from https://CRAN.R-project.org/package=bbmle

Boltaña, S., Rey, S., Roher, N., Vargas, R., Huerta, M., Huntingford, F. A., … Mackenzie, S. (2013). Behavioural fever is a synergic signal amplifying the innate immune response.

Proceedings. Biological Sciences, *280*(1766), 20131381. https://doi.org/10.1098/rspb.2013.1381

Bosch, J., Carrascal, L. M., Durán, L., Walker, S., & Fisher, M. C. (2007). Climate change and outbreaks of amphibian chytridiomycosis in a montane area of Central Spain; is there a link? *Proceedings of the Royal Society of London B: Biological Sciences*, *274*(1607), 253–260. https://doi.org/10.1098/rspb.2006.3713

Brand, M. D., Hill, R. D., Brenes, R., Chaney, J. C., Wilkes, R. P., Grayfer, L., … Gray, M. J. (2016). Water Temperature Affects Susceptibility to Ranavirus. *EcoHealth*, *13*(2), 350–359. https://doi.org/10.1007/s10393-016-1120-1

Breheny, P., & Burchett, W. (2013). *Visualization of Regression Models Using visreg*.

Brunner, J. L., Storfer, A., Gray, M. J., & Hoverman, J. T. (2015). Ranavirus Ecology and Evolution: From Epidemiology to Extinction. In M. J. Gray & V. G. Chinchar (Eds.), *Ranaviruses* (pp. 71–104). Springer International Publishing. https://doi.org/10.1007/978-3-319-13755-1_4

Chen, X., & Tung, K.-K. (2018). Global surface warming enhanced by weak Atlantic overturning circulation. *Nature*, *559*(7714), 387. https://doi.org/10.1038/s41586-018-0320-y

Clare, F. C., Halder, J. B., Daniel, O., Bielby, J., Semenov, M. A., Jombart, T., … Fisher, M. C. (2016). Climate forcing of an emerging pathogenic fungus across a montane multi-host community. *Phil. Trans. R. Soc. B*, *371*(1709), 20150454. https://doi.org/10.1098/rstb.2015.0454

Cohen, J. M., Civitello, D. J., Venesky, M. D., McMahon, T. A., & Rohr, J. R. (2018). An interaction between climate change and infectious disease drove widespread amphibian declines. *Global Change Biology*, 1–11. https://doi.org/10.1111/gcb.14489

Cohen, J. M., Venesky, M. D., Sauer, E. L., Civitello, D. J., McMahon, T. A., Roznik, E. A., & Rohr, J. R. (2017). The thermal mismatch hypothesis explains host susceptibility to an emerging infectious disease. *Ecology Letters*, *20*(2), 184–193. https://doi.org/10.1111/ele.12720

Crawley, M. J. (2013). *The R Book* (2nd Edition). John Wiley & Sons, Ltd.

Cunningham, A. A. (2001). *Investigations into mass mortalities of the common frog (Rana temporaria) in Britain: Epidemiology and aetiology*. Royal Veterinary College (University of London). Retrieved from http://ethos.bl.uk/OrderDetails.do?uin=uk.bl.ethos.269010

Cunningham, A. A., Hyatt, A. D., Russell, P., & Bennett, P. M. (2007). Emerging epidemic diseases of frogs in Britain are dependent on the source of ranavirus agent and the route of exposure. *Epidemiology and Infection*, *135*(7), 1200–1212. https://doi.org/10.1017/S0950268806007679

Cunningham, A. A., Langton, T. E. S., Bennett, P. M., Lewin, J. F., Drury, S. E. N., Gough, R. E., & MacGregor, S. K. (1996). Pathological and microbiological findings from incidents of

669 unusual mortality of the common frog (Rana temporaria). *Philosophical Transactions of the*
670 *Royal Society of London Series B-Biological Sciences*, *351*(1347), 1539–1557.
671 *https://doi.org/10.1098/rstb.1996.0140*

672 Dobson, A., Molnár, P. K., & Kutz, S. (2015). Climate change and Arctic parasites. *Trends in*
673 *Parasitology*, *31*(5), 181–188. *https://doi.org/10.1016/j.pt.2015.03.006*

674 Duffus, A. L. J. (2009). *Ranavirus ecology in common frogs (Rana Temporaria) from United*
675 *Kingdom: Transmission dynamics, alternate hosts and host-strain interactions.* (Thesis).
676 Retrieved from *http://qmro.qmul.ac.uk/jspui/handle/123456789/464*

677 Duffus, A. L. J., Nichols, R. A., & Garner, T. W. J. (2013). Investigations into the life history
678 stages of the common frog (Rana temporaria) affected by an amphibian ranavirus in the
679 United Kingdom. *Herpetological Review*, *44*(2), 260–263. Retrieved from
680 *http://qmro.qmul.ac.uk/xmlui/handle/123456789/10794*

681 Duffus, A. L. J., Nichols, R. A., & Garner, T. W. J. (2014). Experimental evidence in support of
682 single host maintenance of a multihost pathogen. *Ecosphere*, *5*(11), 142.
683 *https://doi.org/10.1890/ES14-00074.1*

684 Elliot, S. L., Blanford, S., & Thomas, M. B. (2002). Host-pathogen interactions in a varying
685 environment: Temperature, behavioural fever and fitness. *Proceedings. Biological Sciences*,
686 *269*(1500), 1599–1607. *https://doi.org/10.1098/rspb.2002.2067*

687 Engering, A., Hogerwerf, L., & Slingenbergh, J. (2013). Pathogen–Host–Environment
688 interplay and disease emergence. *Emerging Microbes & Infections*, *2*(2), e5.
689 *https://doi.org/10.1038/emi.2013.5*

690 Epstein, P. R. (2001). Climate change and emerging infectious diseases. *Microbes and*
691 *Infection*, *3*(9), 747–754. *https://doi.org/10.1016/S1286-4579(01)01429-0*

692 Farrer, R. A., Weinert, L. A., Bielby, J., Garner, T. W. J., Balloux, F., Clare, F., … Fisher, M. C.
693 (2011). Multiple emergences of genetically diverse amphibian-infecting chytrids include a
694 globalized hypervirulent recombinant lineage. *Proceedings of the National Academy of*
695 *Sciences of the United States of America*, *108*(46), 18732–18736.
696 *https://doi.org/10.1073/pnas.1111915108*

697 Garner, T. W. J., Rowcliffe, J. M., & Fisher, M. C. (2011). Climate change, chytridiomycosis or
698 condition: An experimental test of amphibian survival. *Global Change Biology*, *17*(2), 667–
699 675. *https://doi.org/10.1111/j.1365-2486.2010.02272.x*

700 Grassly, N. C., & Fraser, C. (2006). Seasonal infectious disease epidemiology. *Proceedings of*
701 *the Royal Society of London B: Biological Sciences*, *273*(1600), 2541–2550.
702 *https://doi.org/10.1098/rspb.2006.3604*

703 Gray, M. J., Miller, D. L., & Hoverman, J. T. (2009). Ecology and pathology of amphibian
704 ranaviruses. *Diseases of Aquatic Organisms*, *87*(3), 243–266.
705 *https://doi.org/10.3354/dao02138*

706 Hall, E. M., Goldberg, C. S., Brunner, J. L., & Crespi, E. J. (2018). Seasonal dynamics and
707 potential drivers of ranavirus epidemics in wood frog populations. *Oecologia*, *188*(4),
708 1253–1262. https://doi.org/10.1007/s00442-018-4274-4

709 Harvell, C. D., Mitchell, C. E., Ward, J. R., Altizer, S., Dobson, A. P., Ostfeld, R. S., & Samuel, M.
710 D. (2002). Climate Warming and Disease Risks for Terrestrial and Marine Biota. *Science*,
711 *296*(5576), 2158–2162. https://doi.org/10.1126/science.1063699

712 Hoberg, E. P., & Brooks, D. R. (2015). Evolution in action: Climate change, biodiversity
713 dynamics and emerging infectious disease. *Phil. Trans. R. Soc. B*, *370*(1665), 20130553.
714 https://doi.org/10.1098/rstb.2013.0553

715 Holopainen, R., Honkanen, J., Jensen, B. B., Ariel, E., & Tapiovaara, H. (2011). Quantitation of
716 ranaviruses in cell culture and tissue samples. *Journal of Virological Methods*, *171*(1), 225–
717 233. https://doi.org/10.1016/j.jviromet.2010.11.004

718 Hyatt, A. D., Gould, A. R., Zupanovic, Z., Cunningham, A. A., Hengstberger, S., Whittington, R.
719 J., … Coupar, B. E. H. (2000). Comparative studies of piscine and amphibian iridoviruses.
720 *Archives of Virology*, *145*(2), 301–331. https://doi.org/10.1007/s007050050025

721 IPCC. (2000). *Special Report on Emissions Scenarios*. Retrieved from
722 https://www.ipcc.ch/ipccreports/sres/emission/index.php?idp=0

723 Jancovich, J. K., Davidson, E. W., Parameswaran, N., Mao, J., Chinchar, V. G., Collins, J. P., …
724 Storfer, A. (2005). Evidence for emergence of an amphibian iridoviral disease because of
725 human-enhanced spread. *Molecular Ecology*, *14*(1), 213–224.
726 https://doi.org/10.1111/j.1365-294X.2004.02387.x

727 Jenkins, G., Murphy, J. M., Sexton, D. M., Lowe, J. A., Jones, P., & Kilsby, C. G. (2009). *UK*
728 *Climate Projections: Briefing report.* Met Office Hadley Centre, Exeter, UK. Retrieved from
729 http://ukclimateprojections.metoffice.gov.uk/22530

730 Kearney, M., Shine, R., & Porter, W. P. (2009). The potential for behavioral
731 thermoregulation to buffer "cold-blooded" animals against climate warming. *Proceedings of*
732 *the National Academy of Sciences of the United States of America*, *106*(10), 3835–3840.
733 https://doi.org/10.1073/pnas.0808913106

734 Leung, W. T. M., Thomas-Walters, L., Garner, T. W. J., Balloux, F., Durrant, C., & Price, S. J.
735 (2017). A quantitative-PCR based method to estimate ranavirus viral load following
736 normalisation by reference to an ultraconserved vertebrate target. *Journal of Virological*
737 *Methods*, *249*, 147–155. https://doi.org/10.1016/j.jviromet.2017.08.016

738 Lips, K. R., Diffendorfer, J., Mendelson III, J. R., & Sears, M. W. (2008). Riding the Wave:
739 Reconciling the Roles of Disease and Climate Change in Amphibian Declines. *PLOS Biology*,
740 *6*(3), e72. https://doi.org/10.1371/journal.pbio.0060072

741 Marschner, I. (2011). Glm2: Fitting generalized linear models with convergence problems.
742 *The R Journal*, *3*(2), 12–15.

McMichael, A. J., Woodruff, R. E., & Hales, S. (2006). Climate change and human health: Present and future risks. *Lancet (London, England)*, *367*(9513), 859–869. https://doi.org/10.1016/S0140-6736(06)68079-3

Met Office. (2017a). UKCP09: Met Office gridded land surface climate observations - daily temperature and precipitation at 5km resolution. Retrieved December 1, 2017, from http://catalogue.ceda.ac.uk/uuid/319b3f878c7d4cbfbdb356e19d8061d6

Met Office. (2017b). UKCP09: Met Office gridded land surface climate observations - monthly climate variables at 5km resolution. Retrieved September 2, 2018, from http://catalogue.ceda.ac.uk/uuid/94f757d9b28846b5ac810a277a916fa7

Monagas, W. R., & Gatten, R. E. (1983). Behavioural fever in the turtles Terrapene carolina and Chrysemys picta. *Journal of Thermal Biology*, *8*(3), 285–288. https://doi.org/10.1016/0306-4565(83)90010-4

Monis, P. T., Giglio, S., & Saint, C. P. (2005). Comparison of SYTO9 and SYBR Green I for real-time polymerase chain reaction and investigation of the effect of dye concentration on amplification and DNA melting curve analysis. *Analytical Biochemistry*, *340*(1), 24–34. https://doi.org/10.1016/j.ab.2005.01.046

North, A. C., Hodgson, D. J., Price, S. J., & Griffiths, A. G. F. (2015). Anthropogenic and Ecological Drivers of Amphibian Disease (Ranavirosis). *PLoS ONE*, *10*(6), e0127037. https://doi.org/10.1371/journal.pone.0127037

O'Hanlon, S. J., Rieux, A., Farrer, R. A., Rosa, G. M., Waldman, B., Bataille, A., … Fisher, M. C. (2018). Recent Asian origin of chytrid fungi causing global amphibian declines. *Science*, *360*(6389), 621–627. https://doi.org/10.1126/science.aar1965

Picco, A. M., & Collins, J. P. (2008). Amphibian Commerce as a Likely Source of Pathogen Pollution. *Conservation Biology*, *22*(6), 1582–1589. https://doi.org/10.1111/j.1523-1739.2008.01025.x

Pinheiro, J., Bates, D., DebRoy, S., Sarkar, D., & Team, R. C. (2018). Nlme: Linear and Nonlinear Mixed Effects Models (Version 3.1-137). Retrieved from https://CRAN.R-project.org/package=nlme

Plowright, R. K., Sokolow, S. H., Gorman, M. E., Daszak, P., & Foley, J. E. (2008). Causal inference in disease ecology: Investigating ecological drivers of disease emergence. *Frontiers in Ecology and the Environment*, *6*(8), 420–429. https://doi.org/10.1890/070086

Pounds, J. A., Bustamante, M. R., Coloma, L. A., Consuegra, J. A., Fogden, M. P. L., Foster, P. N., … Young, B. E. (2006). Widespread amphibian extinctions from epidemic disease driven by global warming. *Nature*, *439*(7073), 161–167. https://doi.org/10.1038/nature04246

Price, S. J. (2018). Using R to download CEDA datasets. Retrieved July 16, 2018, from https://2infectious.wordpress.com/2018/03/09/using-r-to-download-ceda-datasets/

779 Price, S. J., Garner, T. W. J., Cunningham, A. A., Langton, T. E. S., & Nichols, R. A. (2016).
780 Reconstructing the emergence of a lethal infectious disease of wildlife supports a key role
781 for spread through translocations by humans. *Proc. R. Soc. B*, *283*(1839), 20160952.
782 *https://doi.org/10.1098/rspb.2016.0952*

783 Price, S. J., Garner, T. W. J., Nichols, R. A., Balloux, F., Ayres, C., Mora-Cabello de Alba, A., &
784 Bosch, J. (2014). Collapse of Amphibian Communities Due to an Introduced Ranavirus.
785 *Current Biology*, *24*(21), 2586–2591. *https://doi.org/10.1016/j.cub.2014.09.028*

786 Price, S. J., Wadia, A., Wright, O. N., Leung, W. T. M., Cunningham, A. A., & Lawson, B. (2017).
787 Screening of a long-term sample set reveals two Ranavirus lineages in British
788 herpetofauna. *PLOS ONE*, *12*(9), e0184768. *https://doi.org/10.1371/journal.pone.0184768*

789 R Core Team. (2017). *R: A language and environment for statistical computing. R Foundation*
790 *for Statistical Computing, Vienna, Austria.* Retrieved from *http://www.R-project.org/*

791 Rachowicz, L. J., Hero, J. M., Alford, R. A., Taylor, J. W., Morgan, J. a. T., Vredenburg, V. T., …
792 Briggs, C. J. (2005). The novel and endemic pathogen hypotheses: Competing explanations
793 for the origin of emerging infectious diseases of wildlife. *Conservation Biology*, *19*(5), 1441–
794 1448. *https://doi.org/10.1111/j.1523-1739.2005.00255.x*

795 Raffel, T. R., Michel, P. J., Sites, E. W., & Rohr, J. R. (2010). What Drives Chytrid Infections in
796 Newt Populations? Associations with Substrate, Temperature, and Shade. *EcoHealth*, *7*(4),
797 526–536. *https://doi.org/10.1007/s10393-010-0358-2*

798 Raffel, T. R., Romansic, J. M., Halstead, N. T., McMahon, T. A., Venesky, M. D., & Rohr, J. R.
799 (2013). Disease and thermal acclimation in a more variable and unpredictable climate.
800 *Nature Climate Change*, *3*(2), 146–151. *https://doi.org/10.1038/NCLIMATE1659*

801 Reed, L. J., & Muench, H. (1938). A Simple Method of Estimating Fifty Per Cent Endpoints.
802 *American Journal of Epidemiology*, *27*(3), 493–497. Retrieved from
803 *http://aje.oxfordjournals.org/content/27/3/493*

804 Rohr, J. R., Dobson, A. P., Johnson, P. T. J., Kilpatrick, A. M., Paull, S. H., Raffel, T. R., …
805 Thomas, M. B. (2011). Frontiers in climate change–Disease research. *Trends in Ecology &*
806 *Evolution*, *26*(6), 270–277. *https://doi.org/10.1016/j.tree.2011.03.002*

807 Rohr, J. R., Raffel, T. R., Romansic, J. M., McCallum, H., & Hudson, P. J. (2008). Evaluating the
808 links between climate, disease spread, and amphibian declines. *Proceedings of the National*
809 *Academy of Sciences*, *105*(45), 17436–17441. *https://doi.org/10.1073/pnas.0806368105*

810 Rojas, S., Richards, K., Jancovich, J. K., & Davidson, E. W. (2005). Influence of temperature on
811 Ranavirus infection in larval salamanders Ambystoma tigrinum. *Diseases of Aquatic*
812 *Organisms*, *63*(2-3), 95–100. *https://doi.org/10.3354/dao063095*

813 Rosa, G. M., Sabino-Pinto, J., Laurentino, T. G., Martel, A., Pasmans, F., Rebelo, R., … Bosch, J.
814 (2017). Impact of asynchronous emergence of two lethal pathogens on amphibian
815 assemblages. *Scientific Reports*, *7*, 43260. *https://doi.org/10.1038/srep43260*

816 Sauer, E. L., Fuller, R. C., Richards-Zawacki, C. L., Sonn, J., Sperry, J. H., & Rohr, J. R. (2018).
817 Variation in individual temperature preferences, not behavioural fever, affects
818 susceptibility to chytridiomycosis in amphibians. *Proceedings. Biological Sciences*,
819 *285*(1885). *https://doi.org/10.1098/rspb.2018.1111*

820 Schloegel, L. M., Daszak, P., Cunningham, A. A., Speare, R., & Hill, B. (2010). Two amphibian
821 diseases, chytridiomycosis and ranaviral disease, are now globally notifiable to the World
822 Organization for Animal Health (OIE): An assessment. *Diseases of Aquatic Organisms*, *92*(2-
823 3), 101–108. *https://doi.org/10.3354/dao02140*

824 Schloegel, L. M., Picco, A. M., Kilpatrick, A. M., Davies, A. J., Hyatt, A. D., & Daszak, P. (2009).
825 Magnitude of the US trade in amphibians and presence of Batrachochytrium dendrobatidis
826 and ranavirus infection in imported North American bullfrogs (Rana catesbeiana).
827 *Biological Conservation*, *142*(7), 1420–1426. *https://doi.org/10.1016/j.biocon.2009.02.007*

828 Seimon, T. A., Seimon, A., Daszak, P., Halloy, S. R. P., Schloegel, L. M., Aguilar, C. A., …
829 Simmons, J. E. (2007). Upward range extension of Andean anurans and chytridiomycosis to
830 extreme elevations in response to tropical deglaciation. *Global Change Biology*, *13*(1), 288–
831 299. *https://doi.org/10.1111/j.1365-2486.2006.01278.x*

832 Teacher, A. G. F., Cunningham, A. A., & Garner, T. W. J. (2010). Assessing the long-term
833 impact of Ranavirus infection in wild common frog populations. *Animal Conservation*,
834 *13*(5), 514–522. *https://doi.org/10.1111/j.1469-1795.2010.00373.x*

835 Therneau, T. M. (2018). *Coxme: Mixed Effects Cox Models. R package version 2.2-7.* Retrieved
836 from *https://CRAN.R-project.org/package=coxme*

837 Venables, W. N., & Ripley, B. D. (2002). *Modern Applied Statistics with S* (4th ed.). New York:
838 Springer-Verlag. Retrieved from *//www.springer.com/us/book/9780387954578*

839 Walker, S. F., Bosch, J., Gomez, V., Garner, T. W. J., Cunningham, A. A., Schmeller, D. S., …
840 Fisher, M. C. (2010). Factors driving pathogenicity vs. prevalence of amphibian panzootic
841 chytridiomycosis in Iberia. *Ecology Letters*, *13*(3), 372–382. *https://doi.org/10.1111/j.1461-*
842 *0248.2009.01434.x*

843 Warne, R. W., LaBumbard, B., LaGrange, S., Vredenburg, V. T., & Catenazzi, A. (2016). Co-
844 Infection by Chytrid Fungus and Ranaviruses in Wild and Harvested Frogs in the Tropical
845 Andes. *PLOS ONE*, *11*(1), e0145864. *https://doi.org/10.1371/journal.pone.0145864*

846 Whitfield, S. M., Geerdes, E., Chacon, I., Ballestero Rodriguez, E., Jimenez, R. R., Donnelly, M.
847 A., & Kerby, J. L. (2013). Infection and co-infection by the amphibian chytrid fungus and
848 ranavirus in wild Costa Rican frogs. *Diseases of Aquatic Organisms*, *104*(2), 173–178.
849 *https://doi.org/10.3354/dao02598*

850 Wickham, H. (2016). *Ggplot2: Elegant Graphics for Data Analysis*. Springer.

851 Winton, J., Batts, W., DeKinkelin, P., LeBerre, M., Bremont, M., & Fijan, N. (2010). Current
852 lineages of the epithelioma papulosum cyprini (EPC) cell line are contaminated with

fathead minnow, Pimephales promelas, cells. *Journal of Fish Diseases*, *33*(8), 701–704. https://doi.org/10.1111/j.1365-2761.2010.01165.x

Wood, S. N. (2003). Thin plate regression splines. *Journal of the Royal Statistical Society: Series B (Statistical Methodology)*, *65*(1), 95–114. https://doi.org/10.1111/1467-9868.00374

Wood, S. N. (2004). Stable and Efficient Multiple Smoothing Parameter Estimation for Generalized Additive Models. *Journal of the American Statistical Association*, *99*(467), 673–686. https://doi.org/10.1198/016214504000000980

Wood, S. N. (2017). *Generalized Additive Models: An Introduction with R, Second Edition*. Chapman and Hall/CRC. https://doi.org/10.1201/9781315370279

Supporting information Appendix S1

Supplementary methods: *In vivo* investigation of dose response and disease progression

Acclimation, housing and husbandry: Common frogs (*Rana temporaria*) were reared from eggs (collected at sites with no history of ranavirosis) through metamorphosis and overwintered once. Thirty individuals were randomly allocated to each of three experimental treatments ("high" dose, "low" dose, and a sham control). They were weighed, transferred to individual 1.6 L plastic boxes with a non-airtight lid, a moist paper substrate, and a plastic plant pot for cover and acclimated to the experimental housing for two days prior to viral exposure. The room was climate controlled with lighting set to a constant 12-hour day/night cycle. Environmental conditions (temperature and humidity) were monitored daily for two weeks prior to and throughout the experiment. Mean temperature in the room was 20.2°C (18.6-21.1°C) and mean humidity was 59% (47-79%). Boxes were rotated daily to ensure there were no persistent effects of location on frog responses. Animals were fed brown crickets on alternate days and cleaned and weighed on every fourth day.

Exposure: Ranavirus isolate RUK13 was passaged three times on confluent fathead minnow (FHM) cells in maintenance medium (EMEM plus 10% FBS plus 1% L-glutamine) and spun at 800g to remove cell debris. Virus titer was calculated using a TCID50 (50% Tissue Culture Infectious Dose) protocol in a 96-well flat-bottomed tissue culture plate. TCID50 for the virus stock was then calculated using the Reed and Muench method (Reed & Muench, 1938). Stock virus and sham media were initially diluted in cell culture medium prior to a second dilution step in aged tap-water to ensure that the inoculum for each treatment contained the same total volume of cell culture medium. Viral titers of inocula were $1 \times 10^{4.6}$ TCID50 mL^{-1} of virus for the high

886 dose treatment and 1 x $10^{3.3}$ TCID50 mL^{-1} for the low dose treatment. Animals were bath-
887 exposed in individual 0.07 L plastic boxes for 7 hours prior to returning individuals to their
888 housing.

889 **Sampling:** Animals were monitored daily and scored for changes in spontaneous behaviour,
890 behaviour during handling (when applicable), food intake, stools, and body condition. Animals
891 were also monitored for signs of disease - including reddening of skin, petechial hemorrhaging,
892 ulceration, bleeding, emaciation and lethargy - as well as other physical changes. Swab samples
893 from the pericloacal region of each animal were collected at day 8 using sterile dry swabs
894 (MWE) by rolling the swab tip forwards and backwards across the cloacal entrance three times.
895 Day 8 after exposure was predicted to be the approximate midpoint of the experiment based on
896 previous infections in adult common frogs (Cunningham, Hyatt, Russell, & Bennett, 2007).
897 Approximately half of the animals remaining in the control and low dose treatments were
898 selected at random for euthanasia by a schedule 1 method for amphibians. Five of the animals in
899 the low dose treatment died overnight prior to euthanasia so eight (of 26) animals were
900 euthanized along with 11 (of 22) control animals. Dead animals were examined within twelve
901 hours of death for skin lesions and abnormalities, and post-mortem pericloacal swabs taken. The
902 carcasses (frozen or within three days of death) were examined post-mortem for signs of disease.
903 Liver and kidney samples (approximately 20mg) and the third toe of right hind-foot were frozen
904 at −20°C for DNA extraction and PCR.

905 **Viral load estimation:** tissue samples (and positive and negative extraction control tissues) were
906 disrupted by beating with 5mm beads at 15Hz for 20s in a Qiagen Tissue Lyser II. The tips of
907 swabs were cut off using a new scalpel blade for each sample and placed in individual
908 microcentrifuge tubes with the Promega Wizard digestion mix plus 0.03-0.04g of 0.5mm silica
909 microbeads and beaten for 45s at 30Hz in the tissue lyser alongside extraction controls. All

samples were digested overnight for 18 hours at 56°C prior to extraction with a Promega Wizard SV96 Genomic DNA Purification kit according to the manufacturer's guidelines. DNA was eluted in a single step leading to a total volume of approximately 250µL. DNA concentrations were measured using on a NanoDrop 2000 spectrophotometer.

A quantitative polymerase chain reaction was used to estimate viral load. Primers from Holopainen, Honkanen, Jensen, Ariel, & Tapiovaara (2011) were used to amplify a 93bp fragment of the largest DNA polymerase subunit. SYTO13 was used as the dsDNA reporter dye (Monis, Giglio, & Saint, 2005). Each sample was screened in duplicate wells using a reaction mix of 12.5µL of Promega GoTaq Hot Start Colorless Mastermix, 0.625µL of 10µM forward primer, 0.625µL of 10µM reverse primer, 0.25µL SYTO13 (500µM stock), 0.5µL ROX, 5.5µL of nuclease free water and 5µL of template DNA. Samples were run on 96-well plates with negative controls (duplicate wells with nuclease free water as template) and standards. Standards were generated from a cultured stock of ranavirus isolate RUK11 (Cunningham, Hyatt, Russell, & Bennett, 2007) - quantified following the same protocol described above for RUK13, prior to DNA extraction of a 300µL aliquot of stock virus with a DNAeasy Blood and Tissue spin column following the manufacturer's protocol for 'Purification of Total DNA from Animal Blood or Cells'. Standards were added to each plate in a dilution series in duplicates. Plates were run on an Applied Biosystems Step One Plus thermocycler using the same settings as Holopainen et al. (2011). If one of the replicates failed to amplify or there were large standard deviations of mean CT values samples were rerun in duplicate. Baselines for background fluorescence, thresholds for calculation of CT scores, and exclusion of samples with unusual amplification or melt curves was performed using the AB Step One Plus software. Standard curves were checked to ensure R^2 scores greater than 0.99 and efficiency scores in the range 80-

120%. To account for differences in extraction efficiency, virus quantity scores were standardized by dividing by the concentration of DNA in each sample extract.

Analyses: Associations between signs of disease and exposure to ranavirus (low and high dose combined) were tested using Fisher's exact tests in R. The effect of dose on the amount of virus in tissues of dead animals was investigated using a linear mixed-effects (LME) model with dose and sample type (liver, kidney, toeclip) as fixed effects and individual id as a random effect to account for repeated measures (multiple tissues) from the same individuals [function *lme*, R package *nlme*; Pinheiro, Bates, DebRoy, Sarkar, & R Core Team (2018)]. Viral loads at death were compared to viral loads in live animals using individuals sampled by swabbing between days 7 and 9 post-exposure and again at death (LME model with sample time (alive/dead) as a fixed effect and individual id as a random effect) as well as sets of animals that either died due to disease or were euthanized part-way through the experiment (LME model with the fate of individuals [euthanized/died] as a fixed effect and id as a random effect). The effect of dose on viral loads in all animals swabbed between days 7 and 9 post-exposure was assessed using a linear model. The effect of dose on the timing of signs of disease (disease progression, measured as the first day following exposure that a sign was observed in an individual) was analyzed using a generalized mixed-effects model [Poisson family; *glmer* function in the R package *lme4*; Bates, Mächler, Bolker, & Walker (2015)] with dose and the type of sign as fixed effects and individual as a random effect.

Supplementary references

Bates, D., Mächler, M., Bolker, B., & Walker, S. (2015). Fitting Linear Mixed-Effects Models Using lme4. Journal of Statistical Software, 67(1), 1–48. *https://doi.org/10.18637/jss.v067.i01*

955 Cunningham, A. A., Hyatt, A. D., Russell, P., & Bennett, P. M. (2007). Emerging epidemic
956 diseases of frogs in Britain are dependent on the source of ranavirus agent and the route of
957 exposure. Epidemiology and Infection, 135(7), 1200–1212.
958 *https://doi.org/10.1017/S0950268806007679*

959 Holopainen, R., Honkanen, J., Jensen, B. B., Ariel, E., & Tapiovaara, H. (2011). Quantitation of
960 ranaviruses in cell culture and tissue samples. Journal of Virological Methods, 171(1), 225–233.
961 *https://doi.org/10.1016/j.jviromet.2010.11.004*

962 Monis, P. T., Giglio, S., & Saint, C. P. (2005). Comparison of SYTO9 and SYBR Green I for
963 real-time polymerase chain reaction and investigation of the effect of dye concentration on
964 amplification and DNA melting curve analysis. Analytical Biochemistry, 340(1), 24–34.
965 *https://doi.org/10.1016/j.ab.2005.01.046*

966 Pinheiro, J., Bates, D., DebRoy, S., Sarkar, D., & R Core Team. (2018). nlme: Linear and
967 Nonlinear Mixed Effects Models (Version 3.1-137). Retrieved from *https://CRAN.R-*
968 *project.org/package=nlme*

969 Reed, L. J., & Muench, H. (1938). A Simple Method of Estimating Fifty Per Cent Endpoints.
970 *American Journal of Epidemiology*, *27*(3), 493–497. Retrieved from
971 *http://aje.oxfordjournals.org/content/27/3/493*

Supporting information Appendix S2

Supplementary methods: Proportion of incidents in Frog Mortality Project (FMP) database classified as ranavirosis-consistent

The FMP database contained variables describing the month and year that mortality incidents began as well as georeferences (latitude and longitude on the WGS84 datum; coordinate reference system, EPSG:4326). Monthly averages of the daily maximum temperature for all UK 5 x 5 km grid squares covering the study period (1991 - 2010) were downloaded from the Met Office UKCP09 dataset (Met Office, 2017). All individual points from the FMP database were overlaid on the grid of 5 x 5 km grid squares to retrieve the average local maximum temperature at the onset of each mortality incident.

Supplementary references

Met Office. (2017). UKCP09: Met Office gridded land surface climate observations - daily temperature and precipitation at 5km resolution. Retrieved December 1, 2017, from *http://catalogue.ceda.ac.uk/uuid/319b3f878c7d4cbfbdb356e19d8061d6*

Supporting information Appendix S3

Supplementary methods: *In vivo* investigation of effect of temperature on virulence

In order to validate results from cell culture models *in vivo*, 60 common frogs (*Rana temporaria*) were reared from eggs (collected at sites with no history of ranavirosis) through metamorphosis and overwintered once. Frogs were randomly allocated to one of six treatments (10 animals per treatment); three exposure treatments (sham, RUK11, RUK13) each at two temperatures (20°C and 27°C). The animals were individually housed in 0.7 L volume polypropylene boxes with lids which contained moist paper towels and half a plastic plant pot for cover. Frogs were weighed then acclimated to their boxes at the two incubation temperatures for 72 hours prior to the start of the experiment. They were fed on approximately six small crickets twice weekly after the paper towel substrates had been replaced. During acclimation and throughout the experiment, animals were subjected to a twelve-hour day-night cycle.

Climate controlled chambers were constructed from polystyrene boxes by installing thermostat-controlled heat mats covered in a layer of vermiculite to distribute heat evenly and computer fans to aid air flow. Large rectangular holes were cut in one side of each polystyrene box and covered inside and out with Perspex sheets to create double-glazed windows which let light in whilst insulating against heat transfer. Fifteen frogs in their individual boxes were housed in each polystyrene box along with an additional (identical) box containing an iButton temperature logger (Measurement Systems Ltd, UK) programmed to log the temperature at 30-minute intervals for the duration of the experiment. Boxes were stacked two or three high at the start of the experiment and raised above the heat mat on wire baking trays with space around each stack for airflow. Four polystyrene boxes - two at the “high” temperature (27°C) and two at the “low”

1010 temperature (20°C) - were used with each climate chamber containing five animal boxes from
1011 each of the three exposure treatments. Temperatures in all four climate chambers were stable
1012 around the set points [mean temperatures (standard deviation): Chamber 1 = 26.7 (0.72),
1013 Chamber 2 = 26.5 (0.47), Chamber 3 = 19.9 (0.21), Chamber 4 = 19.9 (0.21)] but were subject
1014 to daily, short-term fluctuations coinciding with removing chamber lids to perform checks
1015 (Figure S1).

1016 The viral inocula were generated by expanding each isolate in EPC cells at 27°C and titers
1017 estimated using TCID50 (Reed & Muench, 1938). Sham exposure inoculum consisted of
1018 supernatant from EPC culture media (Eagle's minimum essential media supplemented with 10%
1019 fetal bovine serum and 1% L-glutamine) with cells removed by centrifugation for ten minutes at
1020 800g. Titers of the two virus isolates were not equalized; RUK13 was used at 1.58×10^5 TCID50
1021 mL^{-1} and RUK11 at 1.58×10^7 TCID50 mL^{-1}. Animals were transferred to 0.07 L polypropylene
1022 boxes which allowed animals to move around but prevented them from climbing. Boxes were
1023 individually numbered, and individuals allocated to treatments according to a random number
1024 draw without replacement made ahead of time using R. The inoculum - 10 mL volume sufficient
1025 to cover the base of the box and ensure that an animal's ventrum was always in contact with the
1026 media - was added by pipetting through a hole in the lid. All animals were subjected to a six-
1027 hour exposure period at room temperature before being returned to their boxes in the climate-
1028 controlled chambers. Individuals were monitored twice daily for signs of disease for the entire
1029 duration of the experiment. Investigators were not blinded to temperature treatment but were
1030 blinded to exposure treatment by using coded IDs. Individuals reaching humane endpoints and
1031 all surviving individuals at the end of the experiment (day eight post-exposure) were euthanized
1032 following a schedule 1 method for amphibians. The number of hours post-exposure that animals
1033 were found dead or at endpoints were recorded for survival analysis.

Supplementary references

Reed, L. J., & Muench, H. (1938). A Simple Method of Estimating Fifty Per Cent Endpoints. *American Journal of Epidemiology*, *27*(3), 493–497. Retrieved from *http://aje.oxfordjournals.org/content/27/3/493*

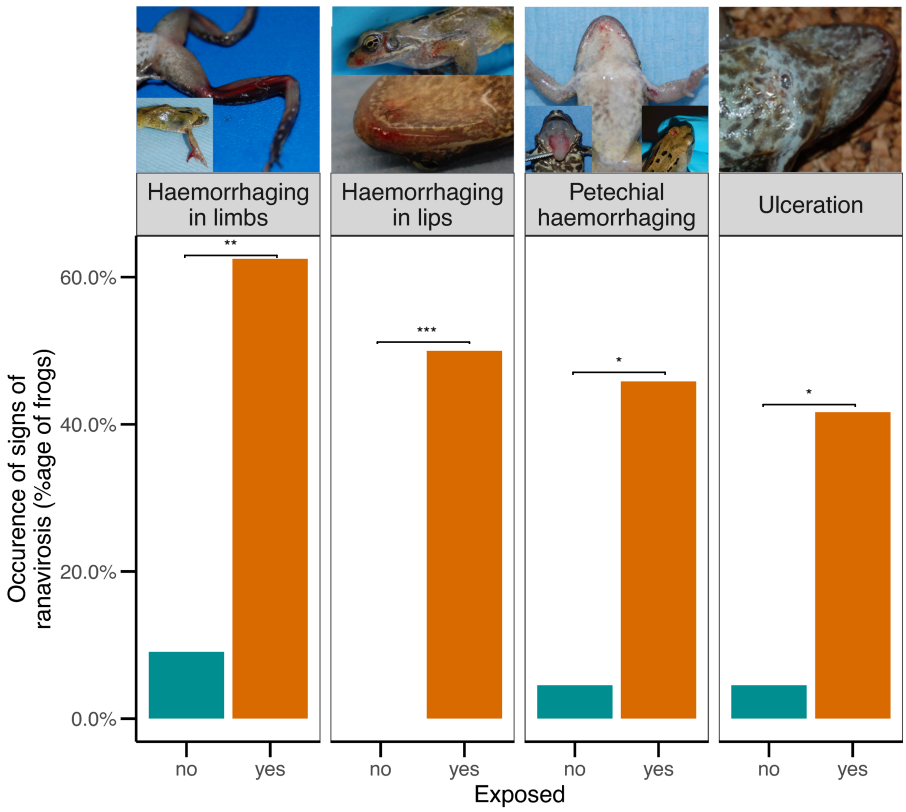

1039

1040 **Figure S1. Association of pathologies with exposure to ranavirus.** Each panel shows the
1041 proportion of experimental animals with observations of signs of disease when juvenile common
1042 frogs (Rana temporaria) were exposed to "low" and "high" doses of ranavirus isolate RUK13
1043 ("exposed") as well as a sham control. Asterisks (*) above plots represent p-values from Fisher's
1044 exact tests of association of signs with exposure treatment: * - $0.01<p<0.05$; ** - $0.001<p<0.01$;
1045 *** - $p<0.001$). A subset of pathologies expected to be identifiable by untrained citizen scientists
1046 were selected, plotted and are represented in the photographs above plots.

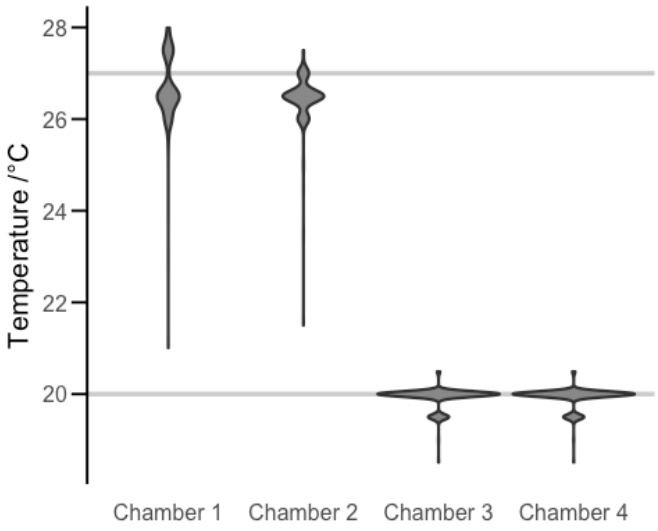

Figure S2. Temperature distribution in each of four climate-controlled chambers across the duration of the *in vivo* temperature experiment. The horizontal lines at 20°C and 27°C show the set points for chambers.

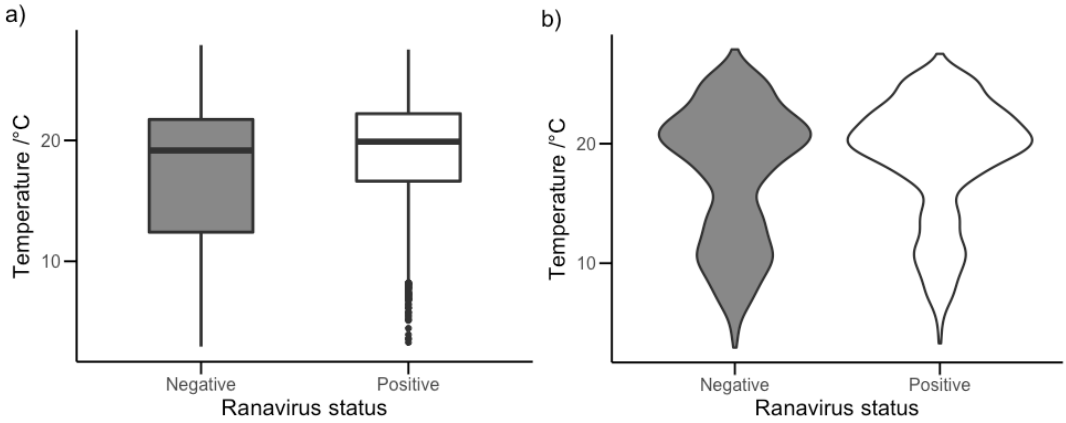

Figure S3. Temperature distribution (average daily maximum temperature) in month of onset of frog mortality for ranavirosis incidents compared to those caused by other factors. Plots comparing distributions: a) Boxplot (lower quartile, median, upper quartile and interquartile range (upper quartile - lower quartile; central 50% of the data); whiskers extend to the most extreme data point which is no more than 1.5 times the interquartile range from the box; outliers shown as individual points). b) Violin plot.

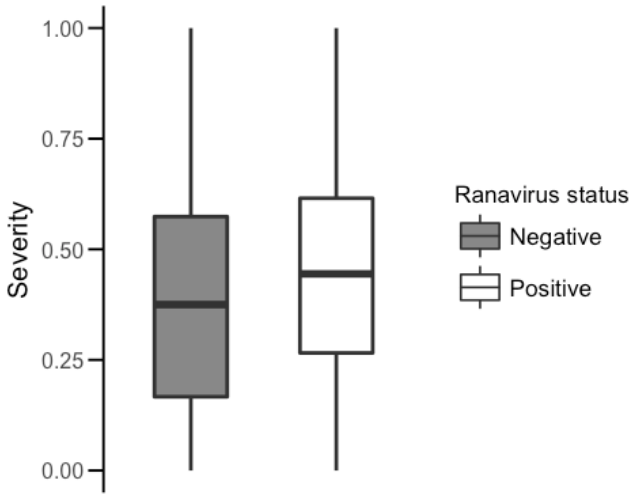

Figure S4. Severity (estimated proportion of population that died) of mortality incidents caused by ranavirus was higher than for those caused by other factors. Boxes represent lower quartile, median, upper quartile and interquartile range (upper quartile - lower quartile; central 50% of the data); whiskers extend to the most extreme data point which is no more than 1.5 times the interquartile range from the box.

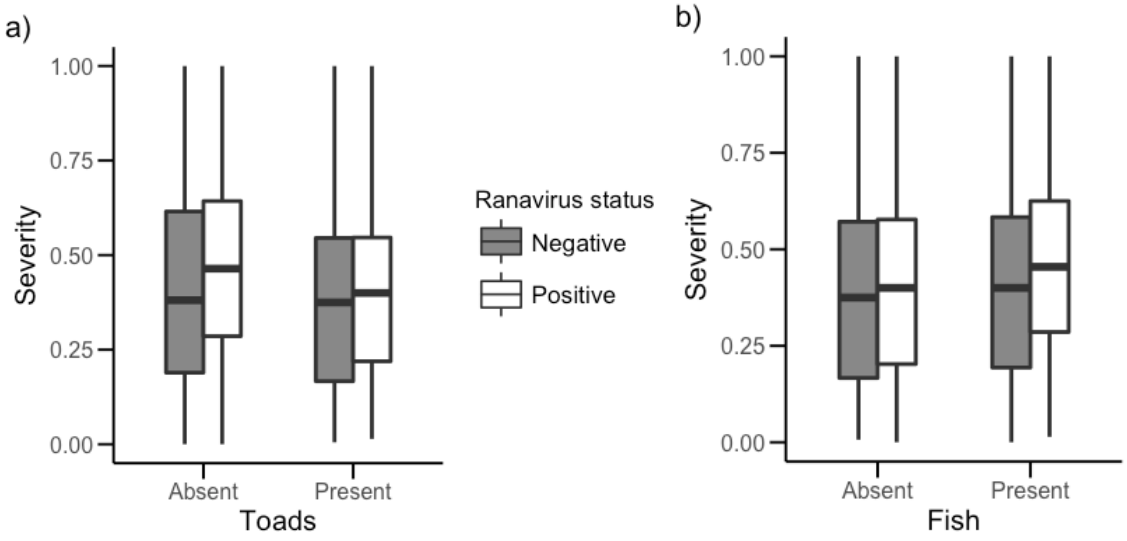

Figure S5. Effect of the presence of other species on the severity (estimated proportion of population that died) of ranavirus outbreaks in common frogs. a) Toads reduced the severity of ranavirus mortality incidents. b) Fish increased the severity of ranavirus mortality incidents. Boxplots represent lower quartile, median, upper quartile and interquartile range (upper quartile - lower quartile; central 50% of the data); whiskers extend to the most extreme data point which is no more than 1.5 times the interquartile range from the box.

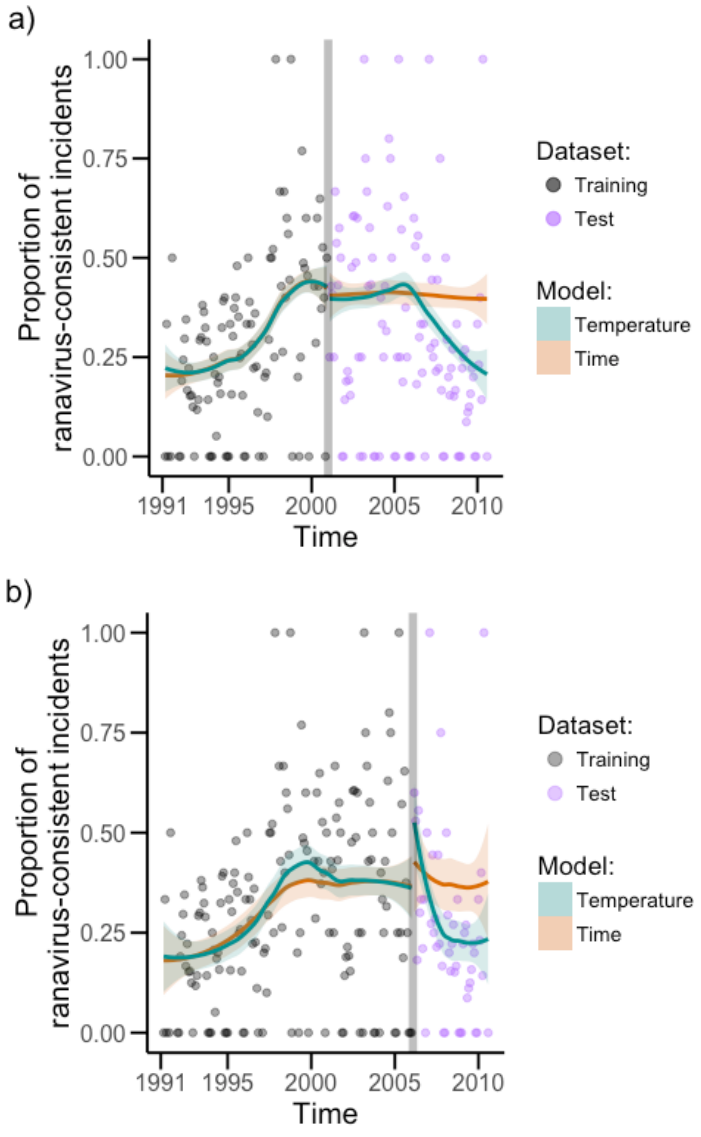

Figure S6. Comparison of power of generalized additive models incorporating either a smoothed time trend or smoothed temperature to predict rates of ranavirosis. a) Models trained on data for 1991-2000 and tested on data for 2001-2010. b) Models trained on data for 1991-2005 and tested on data for 2006-2010. Vertical grey bar represents break between training and test data. Points represent data from the training and test set. Lines are loess smoothed trends predicted from the models with 95% confidence interval shaded.

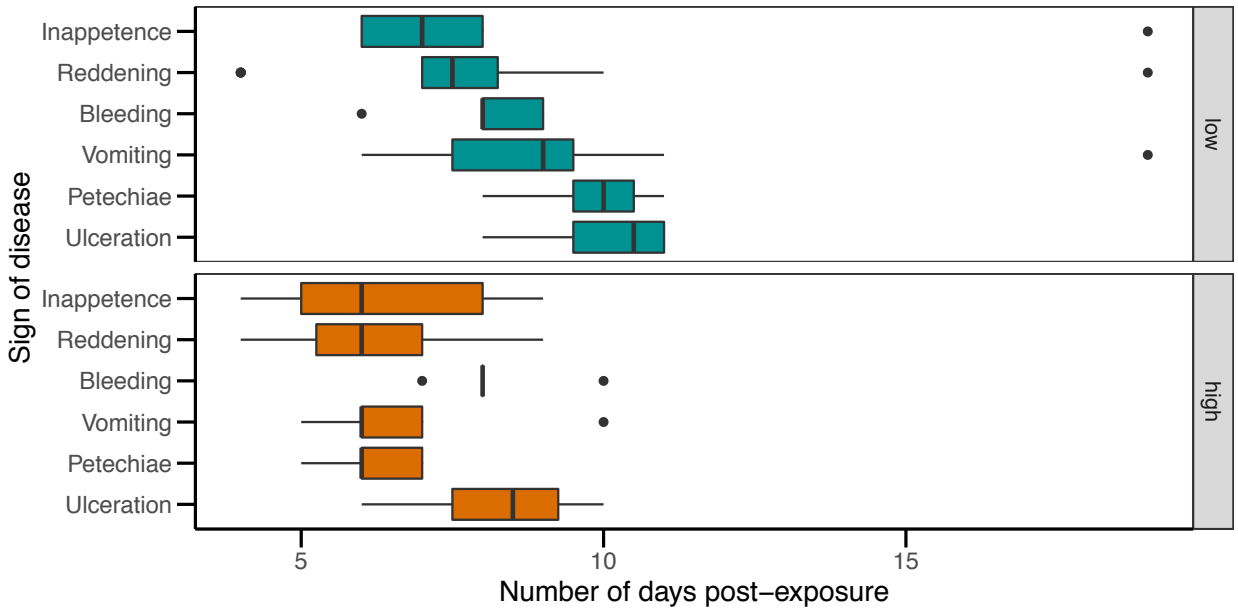

1081

1082 **Figure S7. Effect of exposure dose (high or low) on the timing of signs of ranavirosis.** The
1083 low dose treatment was subject to a significant lag in the onset of disease compared to high dose
1084 (generalized linear mixed-effects model, p= 0.004).

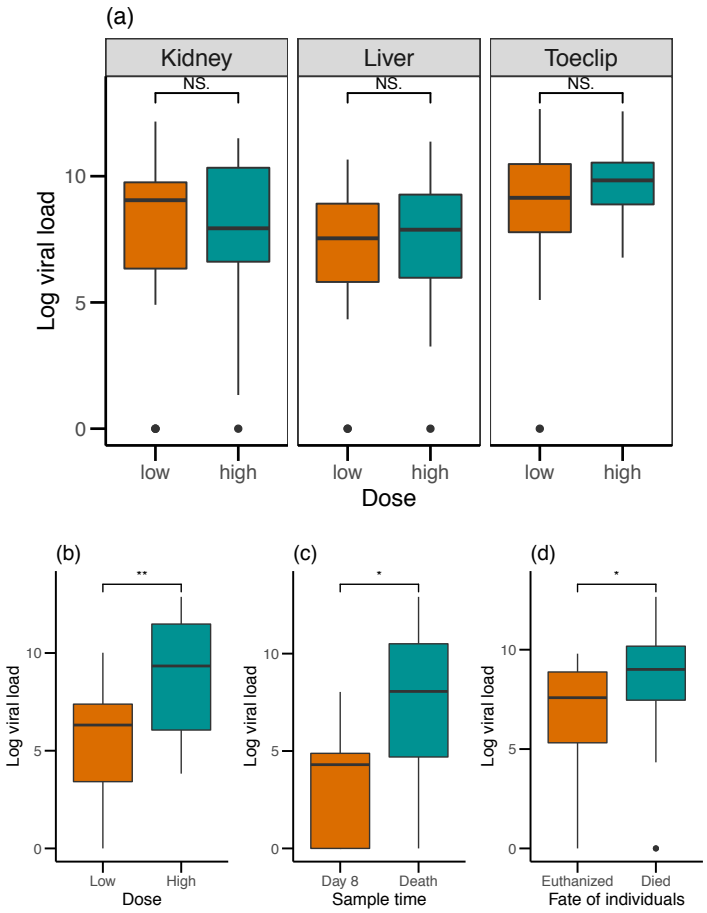

Figure S8. Comparisons of viral load in experimentally infected live and dead common frogs suggested a threshold for disease. (a) At death there is no difference in the viral load in tissues between animals receiving different inoculum doses ($p = 0.51$; linear mixed-effects model with dose and sample type as fixed effects and individual as a random effect), but (b) loads were higher in the high dose treatment at day 8 ($p = 0.006$; linear model, log viral load ~ dose) and increased to death in (c) a subset of animals sampled over time ($p = 0.01$; linear mixed-effects model with sample time as a fixed effect and individual as a random effect) and (d) between animals euthanized at day 8 and those that died ($p = 0.0495$; linear mixed-effects model with fate of individuals [euthanized/died] as a fixed effect and individual as a random effect), suggesting that higher dose increases the initial intensity of infection, giving the virus a head-start, but that all animals reached a threshold viral load that resulted in disease.

Table S1. Model output from logistic model of incidence of ranavirus outbreaks as function of a range of variables describing the local environment of amphibian mortality incidents from Frog Mortality Project reports.

Term	Estimate	Std. Error	z-value	Pr(>|t|)
Intercept	-3.371	0.488	-6.906	<0.001
Av. Max. daily temperature	0.247	0.059	4.225	<0.001
Quadratic term: Av. Max. daily temperature	-0.006	0.002	-3.530	<0.001
Shading (Lots)	-0.278	0.137	-2.029	0.042
Newts (present)	0.268	0.089	3.026	0.002
Fish (present)	0.260	0.099	2.623	0.009

Table S2. Model output from linear model of outbreak severity as function of a range of variables describing the local environment of amphibian mortality incidents from Frog Mortality Project reports.

Term	Estimate	Std. Error	t-value	Pr(>|t|)
Intercept	-1.247	0.365	-3.422	<0.001
Ranavirus status (positive)	-0.615	0.249	-2.470	0.014
Av. Max. daily temperature	0.030	0.004	6.882	<0.001
$\log_2$(pond volume)	-0.075	0.019	-4.063	<0.001
Quadratic term: $\log_2$(pond volume)	0.009	0.002	4.280	<0.001
Shading (Lots)	-0.186	0.067	-2.786	0.005
Marginal vegetation (Lots)	-0.205	0.054	-3.762	<0.001
Toads (present)	-0.209	0.045	-4.658	<0.001
Fish (present)	0.224	0.051	4.381	<0.001
Region 2	0.201	0.377	0.533	0.594
Region 3	-0.185	0.413	-0.449	0.653
Region 4	-0.152	0.397	-0.383	0.701
Region 5	-0.101	0.388	-0.261	0.794
Region 6	0.354	0.360	0.985	0.325
Region 7	0.418	0.360	1.159	0.247
Region 8	0.332	0.358	0.928	0.353
Region 9	0.162	0.365	0.444	0.657
Region 10	0.071	0.477	0.149	0.882
Region 11	-0.053	1.154	-0.046	0.963
Interactions				
Ranavirus status (positive): Av. max. daily temp	0.043	0.013	3.401	<0.001

Table S3. Model output from GAM component of GAMM to decompose seasonal and across year trends in temperature data for study region from 1991 to 2010.

a) parametric component

term	Estimate	Std. Error	t value	Pr(>|t|)
Intercept	14.855	0.116	127.72	<0.001

a) Smoothed component

term	edf	Ref.df	F	p-value
s(month)	7.018	8.000	272.033	<0.001
s(time)	2.361	2.361	2.786	0.048

Table S4. Model output from GAM component of GAMM to decompose seasonal and across year trends in ranavirosis data from 1991 to 2010.

a) parametric component

term	Estimate	Std. Error	t value	Pr(>|t|)
Intercept	0.272	0.014	19.017	<0.001

a) Smoothed component

term	edf	Ref.df	F	p-value
s(month)	4.966	8.000	7.583	<0.001
s(time)	2.974	2.974	7.078	<0.001

Table S5. Model output from Generalized Additive Model of ranavirosis rate as a function of season, time and the across-year trend in temperature.

a) parametric component

term	Estimate	Std. Error	z value	Pr(>|z|)
Intercept	-0.632	0.099	-6.387	<0.001
time	-0.003	0.001	-4.233	<0.001

b) Smoothed component

term	edf	Ref.df	Chi.sq	p-value
s(month)	7.648	8.000	73.629	<0.001
s(temptrend)	6.647	7.379	137.952	<0.001

Data S1. RData file containing all data tables used in analyses.

Data S2. Plain text R file containing code required to run analyses.

Data S3. Viral growth *in vitro* dataset (CSV file).

Data S4. Raw data from data loggers in climate chambers used for *in vivo* test of effect of temperature (CSV file).

Data S5. Frog Mortality Project dataset (CSV file).

Data S6. Ranavirosis outbreaks in wild confirmed by molecular methods dataset (CSV file).

Data S7. Raw room temperature data for *in vivo* test of effect of temperature (CSV file).

Data S8. Survival data from *in vivo* test of effect of temperature (CSV file).